DOI: 10.1070/RCR4807

Porous carbon-based adsorption systems for natural gas (methane) storage

Aslan Yu. Tsivadze,[a] Oleg E. Aksyutin,[b] Alexander G. Ishkov,[b] Ilya E. Men'shchikov,[a] Anatoly A. Fomkin,[a] Andrey V. Shkolin,[a] Elena V. Khozina,[a] Vladimir A. Grachev [a]

[a] A.N.Frumkin Institute of Physical Chemistry and Electrochemistry, Russian Academy of Sciences Leninsky prosp. 31, stroenie 4, 119071 Moscow, Russian Federation
[b] Public Joint Stock Company Gazprom ul. Nametkina 16, 117997 Moscow, Russian Federation

The use of gas fuel has considerable environmental advantages over traditional types of fuel based on petroleum products or fossil coal. The adsorption technology for methane (natural gas) uptake, storage and transportation can serve as a connecting link in gas supply to customers. The review considers characteristics of adsorption systems for methane storage. The key methods used for the synthesis of microporous carbon adsorbents based on various organic and inorganic carbon-containing compounds are described. Methods for increasing the efficiency of methane storage systems based on carbon adsorbents are analyzed. Theoretical approaches to optimization of the properties of methane – carbon adsorbent systems are discussed.
The bibliography includes 174 references.

Contents

1. Introduction 950
2. Key characteristics of adsorption systems for methane storage 953
3. Microporous carbon adsorbents 956
4. Increase in the efficiency of adsorption methane storage systems based on carbon adsorbents 967
5. Theoretical approaches to optimization of the properties of methane – carbon adsorbent adsorption systems 972
6. Conclusion 979

1. Introduction

The use of oil refining products as fuels for portable power sources and for consumers remote from gas mains is going to become problematic in the future. Depletion of large oil deposits necessitates the exploration of oil in new, hard-to-reach areas (in particular, in the Arctic shelf) and application of more complex recovery techniques.[1] This increases the production cost and, correspondingly, affects the consumer prices. Thus, the question arises whether oil refining products would be suitable as energy sources in the future, and the problems of application of alternative fuels, first of all for portable power sources, are brought to the forefront.

Currently, gas fuels (hydrogen, methane, propane – butane mixture) are considered to be most promising, as their utilization in generators and internal combustion engines

A.Yu.Tsivadze. Academician, Doctor of Chemical Sciences, Chief Scientific Adviser of the IPCE RAS.
Telephone: +7(495)952 – 5681, e-mail: tsiv@phyche.ac.ru
O.E.Aksyutin. Doctor of Technical Sciences, Member of the Management Committee, Head of Department of the PJSC Gazprom.
Telephone: +7(495)719 – 3010, e-mail: O.Aksiutin@adm.gazprom.ru
A.G.Ishkov. Doctor of Chemical Sciences, Deputy Head of Department for Gas Transportation, Underground Storage and Use, Head of the Energy Conservation and Ecology Administration of the PJSC Gazprom.
Telephone: +7(495)719 – 3010, e-mail: A.Ishkov@adm.gazprom.ru
I.E.Men'shchikov. Researcher at the Laboratory of Sorption Processes of the IPCE RAS.
Telephone: +7(495)952 – 5681, e-mail: i.menschikov@mail.ru
A.A.Fomkin. Doctor of Physical and Mathematical Sciences, Professor, Head of the same Laboratory.
Telephone: +7(495)952 – 5681, e-mail: fomkinaa@mail.ru
A.V.Shkolin. Candidate of Chemical Sciences, Leading Researcher at the same Laboratory.
Telephone: +7(495)952 – 5681, e-mail: shkolin@bk.ru
E.V.Khozina. Candidate of Physical and Mathematical Sciences, Senior Researcher at the same Laboratory.
Telephone: +7(495)952 – 5681, e-mail: Elena-khozina@rambler.ru
V.A.Grachev. Corresponding Member of the RAS, Doctor of Technical Sciences, Chief Researcher at the Laboratory of Highly Concentrated Disperse Systems of the IPCE RAS.
Telephone: +7(495)952 – 5681, e-mail: vagrachev@gmail.com
Current research interests of the authors: physical chemistry, adsorption, porous materials, natural gas, low-carbon energy engineering, environmental safety, energy conservation, green chemistry.

Received 26 December 2017
Translation: Z.P.Svitanko

© 2018 Uspekhi Khimii, Russian Academy of Sciences and Turpion Ltd.

has been technically implemented with relatively high efficiency coefficients. Moreover, as follows from the data of IHS Cambridge Energy Research Associates,[2] the world resources of natural gas would be able to meet the needs of humanity for at least 250 years.

It also seems important that gas fuel offers considerable environmental advantages over traditional liquid fuels based on oil refining products and hard coals. The most important advantages are as follows:[3]

— the gas contains no traces of lead or other heavy metals; therefore, there is no metal emission to the environment;

— exhaust gases contain no solid particulates coming from additives, which could cause respiratory or cardiovascular diseases in humans upon inhalation;

— the content of sulfur is relatively low (according to GOST R 53367-2009, the hydrogen sulfide and mercaptan sulfur contents in the natural gas are 0.02 and 0.036 g m^{-3}) and, as a consequence, emission of sulfur dioxide, which is a typical component of the combustion products of liquid fuels, is considerably lower;

— natural gas combustion gives off less CO (by 76%), NO_x (by 75%), hydrocarbons (by 88%) and CO_2 (by 30%).

The key factor that prevents the extensive use of gas fuel for remote consumers is the lack of energy-efficient, fire and explosion safe systems for gas storage and transportation with high storage capacity. Therefore, during the last decades, intensive research has been in progress with the goal to design new portable gas fuel systems that would compete well with the existing systems using oil refining products.

Natural gas, which mainly consists of methane (70% to 98%), is most promising, among gas fuels, as regards the accessibility and technical implementation. However, extensive application of natural gas in portable fuel systems is hampered by a number of obstacles related to gas uptake in storage and transportation systems.

Currently, systems of compressed and liquefied natural gas are used. The prevalence of compressed gas systems is restricted due to stringent requirements to fire and explosion safety and the necessity to reach high pressures (up to 20 MPa) to increase the storage efficiency. Modern high-pressure compressors are expensive and not sufficiently reliable and the compressed gas systems are heavy-weight, as they have to operate at high pressure. In addition, these systems can store relatively low amounts of natural gas (methane), namely, about 240 m^3 m^{-3} at 20 MPa and 293 K.

Liquefied natural gas systems, which store the gas at slight overpressures, are relatively light-weight and retain considerable amounts of gas (expressed in specific volume units) — approximately 500–560 m^3 m^{-3}. However, in this case, safety requirements are even more stringent than for compressed gas systems. The main factors responsible for the complexity of operation of liquefied natural gas systems as well as their high cost are listed below.[4]

— problems associated with the necessity to vent the vapour formed above the liquefied gas and upon expansion of the liquid;

— spreading of the cooled vapour, which drifts low over the ground and fills hollows;

— discharge of pressurized liquefied methane;

— gas cloud explosions;

— temperature stratification of the liquid giving rise to rollover.

The significance of natural gas (methane) storage and difficulties associated with the use of compressed and liquefied natural gas stimulated numerous scientific studies aimed at the design of storage systems based on a variety of materials.[5] For example, studies of methane solubility carried out at high pressure[6] demonstrated that out of more than 40 solvents, the best ones are n-butane, n-pentane, isopentane and dimethyl ether. Nevertheless, because of the poor solubility of methane, the use of these systems is technically difficult and expensive. The method of methane storage as gas hydrates[7] has not yet found wide use either, because of the low volume of the stored gas and complex conditions of hydrate formation.

Currently, adsorption storage can be distinguished as the most promising technique for natural gas (methane) storage and delivery to the consumer. The advantages of this method are due to the following factors.

1. Gas adsorption and storage occur under ambient (or nearly ambient) conditions, in particular, at temperatures ranging from 233 to 323 K. Hence, there is no need to generate special conditions, as for example, for liquefied natural gas storage or gas hydrate methane storage.

2. The adsorption storage of methane is possible at low pressure (down to 3.5 MPa), which enables simpler and more efficient engineering solutions that decrease energy expenditures for charging, compared with those for compressed gas storage systems, without the loss of storage efficiency. It is also noteworthy that storage of methane in the adsorbed state does not require energy expenditure and is not accompanied by loss of the fuel, which is involved in the use of liquefied gas storage systems. Thus, adsorption systems are presumably fairly energy efficient.

3. Enhanced fire and explosion safety, which are due to a change in methane properties upon adsorption in micropores resulting from interactions between the adsorbate and the porous material in the adsorption force field. The issues of safety of adsorbed methane storage in carbon adsorbents have been discussed in several studies,[8–11] in which the authors do not give any experimental estimates, but agree that relatively simple engineering solutions, allowing natural gas storage at a relatively low pressure (up to 3.5 MPa), ensure a high safety level.

Efficient natural gas (methane) storage is provided by its adsorption in microporous materials. The absence of specific interactions in methane molecules, in particular, electrostatic interactions induced by a dipole or quadrupole moment, results in their adsorption only through dispersion forces, which arise in micropores having high characteristic energies. The microporous materials that deserve mention include carbon adsorbents, synthetic zeolites and silica gels; they are manufactured on an industrial scale and are widely used in various areas. Carbon nanotubes, fullerenes and metal-organic[12,13] and covalent-organic[14] frameworks, which are currently synthesized, as a rule, only in gram quantities, can be considered as prospective microporous materials.

The first studies in the field of adsorption storage of natural gas were undertaken in the last quarter of the 20th century. In 1983, the Ford Motor Company in the USA initiated a research into the adsorption storage of gas fuel for natural gas motor vehicles.[15] The methane adsorptions on activated carbon (9LXC brand) and on molecular sieves

were compared at pressures of up to 16 MPa. Carbon proved to be a better adsorbent for methane than molecular sieves. This result was attributed to the fact that methane molecules with no dipole or quadrupole moment can be sorbed only through van der Waals forces arising inside a micropore, whereas in the zeolite-based molecular sieves, adsorption is mainly due to the presence of cations in the pores, which polarize the gas molecules. Moreover, it was found that the stored gas volume is much higher in a vessel filled with a carbon adsorbent than in a vessel without an adsorbent (a conventional cylinder with compressed natural gas), especially at low pressures. In 1985, the first US patents were granted [16,17] for adsorption-based hydrocarbon fuel storage systems for vehicles. At the same time, studies of the methane adsorption on microporous carbon adsorbents and NaX zeolites were carried out at the Institute of Physical Chemistry of the Academy of Sciences of the USSR.[18] It was shown that the corresponding adsorption isotherms are linear for both types of adsorbents in both subcritical and supercritical ranges of temperature (120–600 K) and pressure (0.1–20 MPa), which provided grounds for potential use of these materials in natural gas storage systems.

In the late 1980s–early 1990s, several publications reported the results of studies of methane adsorption in the micropores of carbon adsorbents [19] and zeolites,[20,21] undertaken in order to determine their optimal properties.[22–25] Among other studies, computer simulation of the adsorption was performed. In particular, Monte Carlo simulation [22] of methane adsorption in the 1.14 nm wide slit-shaped pores of a carbon material was used to determine the optimal pellet size and shape of adsorbent particles. Cracknell *et al.*[24] investigated the effect of geometric parameters of micropores in the carbon- and zeolite-based adsorbents on methane adsorption. The dependences of the adsorption capacity of microporous carbon materials on the activation method and conditions were elucidated in relation to the CNS carbon adsorbent activated using carbon dioxide and the PVDC (polyvinylidene chloride) carbon adsorbent activated by steam.[26] A study of methane adsorption on a KOH-activated carbon material [27] demonstrated that it adsorbed more efficiently than steam-activated carbon materials. The advantage is caused by a larger micropore volume. It was also reasonable to pay attention to the natural gas (methane) desorption from various adsorbents, which determines the delivery of the energy carrier to the consumer. In particular, the effects of temperature and adsorber design on the gas discharge from cylinders filled with the adsorbent were elucidated.[28]

By the end of the 20th century, the number of papers dealing with methane adsorption has increased, but they did not represent systematic research in this field. In the late the 1990s, the US Department of Energy formed a research group called AGLARG, which started working, according to a special research programme, on the design of materials for natural gas (methane) storage under ambient conditions. In the mid-1990s, a requirement to the adsorption capacity of natural gas (methane) storage systems under standard conditions was stated for the first time to be 150 $m^3\ m^{-3}$ (the volume of methane recalculated for the conditions of 273 K and 0.1 MPa, which is stored in the storage system per its unit volume).[29] A pressure of 3.5 MPa and a temperature of 298 K were chosen as reference conditions. Systematic studies devoted to the adsorption storage of natural gas (methane) by various types of adsorbents have been reported. In 2000, the requirement to the adsorption capacity of methane storage systems was increased to 180 $m^3\ m^{-3}$ (Ref. 30), which stimulated the search for fundamentally new materials such as carbon nanotubes,[31] metal-organic frameworks [32] and porous framework polymers.[33]

However, as follows from numerous data presented in an analytical review,[34] the goal set for research groups in 2000 is still relevant. According to authors' estimates, a natural gas (methane) storage system delivering 180 $m^3\ m^{-3}$ to the consumer should have a capacity of at least $\sim$245 $m^3\ m^{-3}$ and the adsorbent packing density should be in the range from 461.5 to 1000 kg m^{-3}.

In 2012, the US Advanced Research Project Agency revised the requirements to methane storage systems:[35] the gravimetric storage capacity for methane should be at least 0.5 g(CH_4) g^{-1} and the specific volumetric capacity for a monolithic block of the adsorbent should be 264–266 $m^3\ m^{-3}$ at 3.5 MPa and 298 K, which is equivalent to compressed methane storage in cylinders at 25 MPa and 298 K. As noted in the review,[34] these requirements refer to the discharge with pressure decrease from 3.5 to 0.1 MPa, *i.e.*, to the amount of the gas that can be extracted from the storage device and delivered to the consumer. This increases the required absolute volumetric capacity for methane storage to $\sim$373 $m^3\ m^{-3}$. Today, this value seems a long term perspective, while researchers engaged in the synthesis of new materials aim, most often, at lower values.

It is noteworthy that, apart from the general requirements to the volumetric and gravimetric capacity, an adsorbent should possess certain adsorption characteristics, in particular: [3]

— energetically optimal relationship between the adsorption and desorption processes, that is, a material with a high adsorption capacity should give off the highest gas volume without forced heating;

— optimal micropore size for gas desorption at room temperature ($\sim$0.8–1.4 nm);

— high packing density that would ensure a decrease in the gas phase volume in the storage system;

— relatively low heat of adsorption at a high heat capacity of the porous material; in this case, it may be possible to decrease thermal oscillations upon the change in the environmental temperature;

— extensive transport porosity for high mass transfer rates;

— hydrophobicity.

Apart from the adsorption properties, an adsorbent should also meet a number of requirements imposed on an operating material, namely, it should possess sufficient strength to rule out dusting caused by attrition of pellets, stability to cyclic mechanical loads, and relatively low cost.

As noted above, a considerable portion of studies on methane storage use microporous carbon adsorbents obtained from various raw materials. Other materials have also been proposed as adsorbents, including zeolites, silica gels, carbon nanotubes, metal-organic frameworks and porous polymers. In numerical simulation experiments for methane storage systems aimed at increasing their energy efficiency, fundamentally new and, in some cases, exotic materials have also been considered such as nanocones, nanocapsules, modified metal-organic and covalent organic

frameworks, carbon nanotube arrays, silicon nanotubes, carbon fibres, porous polymer networks and so on. We would like to note the most comprehensive reviews devoted to methane storage in the adsorbed state.[3, 25, 36 – 48]

In 1998, Menon and Komarneni[25] made the first attempt to integrate the results of experimental and theoretical studies of high-pressure methane adsorption in the most common adsorbents including activated carbons, silica gels and zeolites. However, since data on methane adsorption were scarce, they elucidated only the general dependences of adsorption on the specific surface area, which is considered as the key adsorbent characteristic. Cook *et al.*[36] discussed the engineering aspects of methane storage in adsorption systems and ways of increasing their efficiency including optimization of the design of adsorbers, charge and discharge systems and so on. Later publications of Burchell[37] and Lozano-Castello *et al.*[38] were the first to consider in detail the role of technological compaction of carbon adsorbents. Important results were obtained by comparison of the adsorption – desorption of natural gas as a mixture of components and methane (as one of its components) in various adsorbents.[39] In particular, a linear dependence was obtained for the methane uptake on the adsorbent specific surface area at supercritical temperatures. It was shown that at ambient temperatures, other natural gas components are not always desorbed from the system. This possibility must be taken into account in the calculations of the natural gas storage.[39]

The beginning of the 21st century witnessed the appearance of new materials, metal-organic coordination polymers, and extensive development of theoretical simulation of adsorption by molecular dynamics, Monte Carlo and density functional theory techniques. Actually, a new research area appeared — the design of porous materials, which was reflected in the survey publication of Solar *et al.*[3] In particular, they discussed selection of the porous structure parameters for carbon adsorbents on the basis of micropore shape (tubular or slit-shaped). The same review presents analysis of experimental results on methane adsorption in new materials based on metal-organic structures. Makal *et al.*[40] focused attention on the prospects of metal-organic and covalent organic frameworks and also porous organic polymers as adsorbents for methane storage systems. The key characteristics of virtually all types of porous materials applicable for natural gas storage systems were briefly described by Chang *et al*;[41] however, the authors did not discuss the fundamental regularities of the adsorption storage of methane.

Choi *et al.*,[43] who analyzed the development of on-board adsorption systems for motor vehicles, noted that the success of a technology is determined by the cost/performance ratio of the used materials. Among all materials, carbon adsorbents are regarded as materials of choice, considering the whole set of their technical, cost and performance characteristics. A similar conclusion was drawn in another publication.[42]

Nie *et al.*[44] reported an integrating analysis of the theoretical trends of methane adsorption in various types of porous materials, the properties of the materials and achievements of research groups and commercial companies in the design of real gas storage systems. The researchers also indicated metal-organic structures and carbon materials to be the most promising adsorbents. Their advantages were confirmed in a study[45] on the adsorption storage of methane by carbon samples obtained from various sorts of biomass. The potential applicability of adsorbents based on metal-organic structures and modified carbon materials is also noted in a critical review,[46] which presents the results of measurements of methane adsorption in nanoporous materials.

The most comprehensive review[47] was published in 2017; the authors analyzed the theoretical and experimental data on the fundamental trends of methane adsorption in various materials. The key porous structure parameters (specific surface area and volume of micropores) that affect the efficiency of adsorption gas storage in a particular material were considered in detail. Microporous carbon materials and metal-organic frameworks were also indicated as promising adsorbents for natural gas storage systems.

Thus, considering the above literature sources, it can be concluded that among all available nanoporous materials, carbon adsorbents are the materials of choice for the adsorption storage. However, the above publications do not pay adequate attention to the preparation of adsorbents. A specific feature of the present review is focusing on the engineering aspects of the synthesis of carbon adsorbents and on the results of studying their adsorption characteristics. It also seems necessary to analyze the theoretical approaches to optimization and fine tuning of porous structure parameters of carbon materials for methane storage systems.

The following abbreviations are used in the review:

AC —activated carbon;

AGLARG — Atlanta Gas Light Adsorbent Research Group;

ANG — adsorbed natural gas;

BET — Brunauer – Emmett – Teller;

CNG — compressed natural gas;

CNS —coconut shell;

COF — covalent organic framework;

DOE — US Department of Energy;

HSAC — high-surface activated carbon;

LNG — liquefied natural gas;

NIST — US National Institute of Standards and Technology;

MOF — metal-organic framework;

MSC — maxsorb superactivated carbon;

TVFM — theory of volume filling of micropores;

NTP — normal temperature and pressure;

STP — standard temperature and pressure;

ZTC — zeolite templated carbon.

2. Key characteristics of adsorption systems for methane storage

Microporous adsorbents show the highest adsorption activity towards various gases, including methane; this is due to the mechanism of volume filling of pores inherent in these materials.[48]

The key parameter determining the efficiency of an adsorption storage system is the amount of the target substance (natural gas, methane) stored in the system under particular thermodynamic conditions determined by the pressure (P) and temperature (T). In the general case, total (absolute) adsorption is taken as such a parameter

$$n_a(P,T) = n_e(P,T) + W_0 \rho_g(P,T) \quad (1)$$

where $n_e(P,T)$ is the excess adsorption at the specified parameters P and T; W_0 is the volume of the adsorbent micropores; $\rho_g(P,T)$ is the density of the adsorptive gas at the specified P and T.

While evaluating the integral specific efficiency of an adsorption system representing a vessel filled with an adsorbent, one should consider not only the adsorbed phase of the target gas, but also the free gas phase that occupies the volume free from the adsorbent. In this case, the total specific capacity of the storage system including both the adsorbed and free gas phases is taken as the criterion.

The total volumetric specific capacity of a storage system (V_f) is the total amount of the free and adsorbed phases of the target gas per unit volume of the closed system containing the adsorbent at specified pressure and temperature converted to standard or normal thermodynamic conditions.† The pressure dependence of the total specific capacity of an adsorption system for methane storage with the carbon adsorbent AU-1 at 300 K is presented in Fig. 1.

The V_f value is usually measured in m^3(STP) m^{-3} (according to the IUPAC rules) or in m^3(NTP) m^{-3} according to NIST or to GOST 2939-63[50] in publications of Russian authors.[53] Along with the volumetric specific capacity of a storage system, an equivalent quantity called volumetric storage density is used in the literature.[54] The V_f value is calculated from the relation

$$V_f = V_a(P,T) + V_g(P,T) \quad (2)$$

where V_a and V_g are the total specific gas volumes within a closed system of unit volume containing the adsorbent in the adsorbed and gaseous states at particular P and T values. By expanding the terms of Eqn (2), one gets

$$V_f = n_a(P,T)\mu\frac{d}{\rho} + \varepsilon\frac{\rho_g(P,T)}{\rho} \quad (3)$$

where μ is the molar mass of methane; d is the adsorbent packing density; ρ is the density of the free methane phase at STP or NTP; ε is the porosity (void content) of the adsorbent layer.[55]

The void content, or the fraction of the system volume free from the adsorbent and the adsorbate is calculated from the relation

$$\varepsilon = 1 - \left(W_0 d + \frac{d}{d_{cr}}\right) \quad (4)$$

where d_{cr} is the crystalline density of the material.

As the microporous adsorbent is compressed and its packing density approaches the density of a single pellet,[55] the void content tends to zero. This limiting case is possible, for example, when the adsorbent is prepared and activated as a large monolith.

From the standpoint of operation of an ANG system, an important value is the volumetric active specific capacity of the system (V_d), or deliverable capacity, rather than the total specific capacity. The V_d value is defined as the amount of the gas (converted to the STP or NTP) that can be delivered from the vessel with adsorbent of some volume upon isothermal gas discharge with a pressure drop from the current level to a specified minimum P_x value divided by the geometric volume of the vessel.[45,56] The pressure dependence of the total specific capacity of a methane storage system with the adsorbent AU-1 at 300 K is depicted in Fig. 2.

The P_x values are chosen according to the system operation conditions. In foreign literature sources, P_x is chosen between 0.48 and 0.58 MPa,[47] which corresponds to the minimum operating level for gas delivery to a power facility, for example, to an internal combustion engine. In Russian publications, P_x corresponds to atmospheric pressure.[53] The gas remaining in the system after discharge is called undeliverable, or passive. The active capacity V_d is found as the difference between $V_f(P,T)$ and $V_f(P_x,T)$.[53]

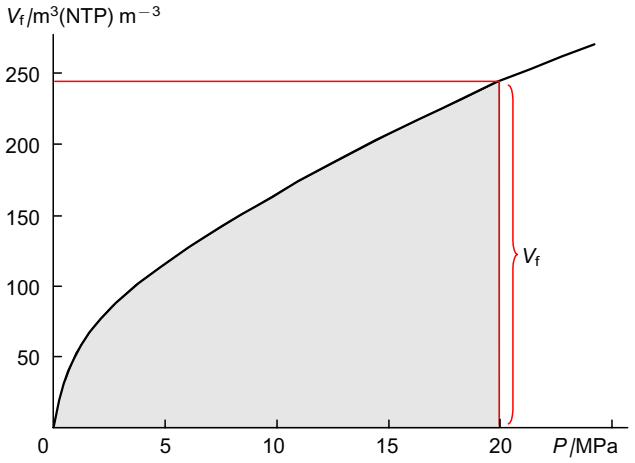


Figure 1. Total specific methane storage capacity of the adsorption system with the adsorbent AU-1 *vs.* pressure at 300 K.[53] The designated area is the total specific capacity in the pressure range from 0 to 20 MPa.

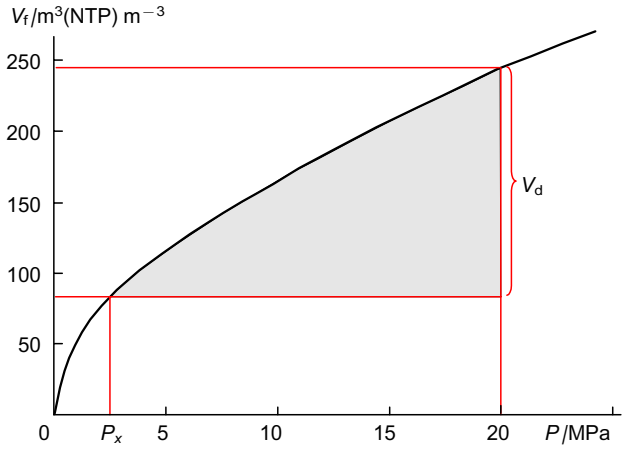


Figure 2. Total specific methane storage capacity of the adsorption system with the adsorbent AU-1 *vs.* pressure at 300 K.[53] The designated area is the deliverable specific capacity in the pressure range from 2.5 to 20 MPa, P_x = 2.5 MPa.

† According to the IUPAC rules, the standard thermodynamic conditions for gases (STP) are T = 273.15 K, P = 101325 Pa;[49] according to NIST, the normal conditions for gas volume determination (NTP) are T = 293.15 K, P = 101325 Pa.[50–52]

When $P_x = 0.1$ MPa, the V_d value can be calculated from the relation:

$$V_d = V_f(P,T) - V_f(P_{0.1},T) \quad (5)$$

Determination of the pore volume for an adsorbent is a challenging task; direct experimental determination of the total adsorption at high pressure requires special equipment.[57] In foreign literature, the capacity characteristics of storage systems are determined using experimental data on excess adsorption.[42] However, in our opinion, this approach is not well-posed, since the n_e and n_a values can substantially differ, especially at high pressures typical of methane storage systems. Therefore, in what follows, we consider the total adsorption.

Technically, the CNG technology resembles most closely the ANG technology; therefore, for evaluation of the efficiency, adsorption systems are often compared with compressed gas systems. In view of this fact, the value of absolute efficiency of an adsorption storage system (ΔV_f) was introduced as the difference between the V_f values of the adsorption system ($V_{f\ ANG}$) and the compressed gas system ($V_{f\ CNG}$) under the same thermodynamic conditions

$$\Delta V_f(P, T) = V_{f\,ANG}(P, T) - V_{f\,CNG}(P, T) \quad (6)$$

As an example, Fig. 3 shows the pressure dependences for the total specific capacity of a methane storage system with the adsorbent AU-1 and the compressed gas system for 300 K.

One more parameter used to compare the ANG and CNG technologies is the relative efficiency of an adsorption storage system. This value is defined as the ratio of the V_f values of the adsorption system and the compressed gas system under identical thermodynamic conditions

$$\eta_v = \frac{V_{f\,ANG}(P, T)}{V_{f\,CNG}(P, T)} \quad (7)$$

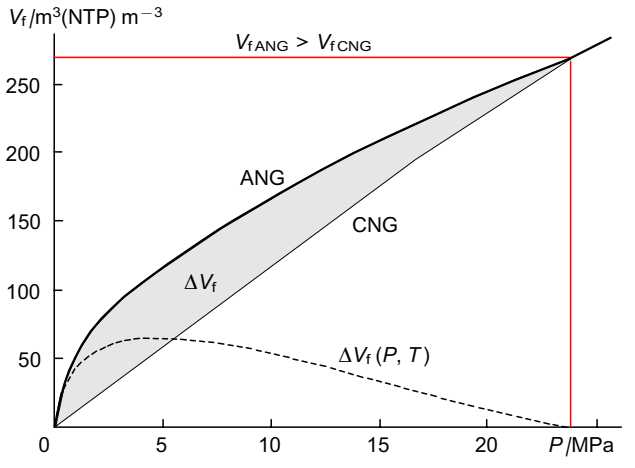


Figure 3. Total specific methane storage capacity of the ANG system with the adsorbent AU-1 and a CNG system *vs.* pressure at 300 K.[53]
The area in which the ANG system surpasses the CNG system is designated.

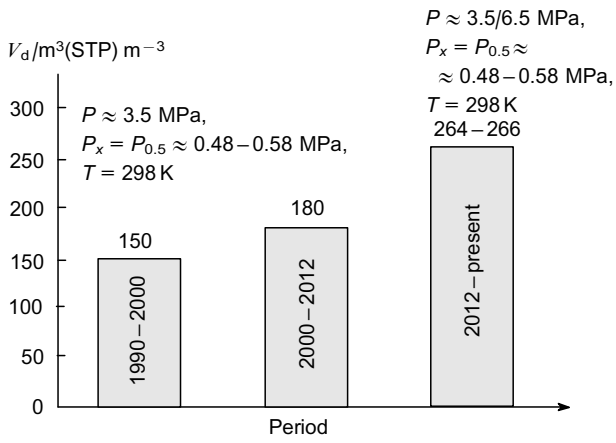


Figure 4. Requirements to the deliverable specific capacity of natural gas (methane) adsorption storage systems formulated by the DOE.[29, 36, 43, 47, 58, 59]

where η_v is the volumetric relative efficiency coefficient for an ANG system.

It should be noted that no theoretically or practically substantiated requirements to V_f and V_d have been developed to date. Nevertheless, the authors of most publications devoted to the adsorption storage of methane refer to the requirements developed by DOE together with the AGLARG group.[29] Figure 4 presents the requirements to the adsorption storage systems and their variation trends.

It can be seen that the requirement to the deliverable capacity of methane storage systems has permanently increased starting from 150 (in 1995) and ending with 264–266 m³(STP) m^{-3} (in 2012). It is important that the requirements to V_d defined in 2000 and 2012 are referred to the specific capacity of CNG systems at pressures of 16.3 and 25 MPa, respectively. Before 2012, the operating pressure of an adsorption system did not exceed 3.5 MPa, but later it was raised to 6.5 MPa (Ref. 60), because of inefficient operation of ANG systems in the pressure region below 3.5 MPa. Apart from the presented volumetric characteristics, it is necessary to indicate the requirement to the gravimetric adsorption capacity, which is 0.5 g (CH_4) g^{-1} (total uptake), developed within the framework of the Methane Opportunities for Vehicular Energy programme (DOE, USA) and published.[61] It is noteworthy that the capacity target set in 2012 corresponds to the value for an CNG system at $P = 25$ MPa.

The thermodynamic parameters of systems presented in Fig. 4 were determined back in 1966 by Peterson *et al.*,[62] who demonstrated that the density of methane adsorbed in PCB type activated carbon at a pressure of 3.6 MPa and a temperature of 298 K exceeds the density of the free methane under the same thermodynamic conditions. This idea was further developed in pioneering studies.[5, 63] The authors of some publications indicated the pressure of ~2.5 MPa, which they considered to be the optimal pressure for achieving the highest energy efficiency of charging ANG systems.[36]

Although most of the researchers are guided by the values presented in Fig. 4, in our opinion, these values are not substantiated by physicochemical properties of high-pressure energetic adsorption systems. Indeed, most of the studies are arranged according to a common principle and

include analysis of the adsorbent porous structure, adsorption measurements and finally calculation of the V_f and V_d values according to the DOE requirements. However, some researchers, in particular, Senkovska and Kaskel[64] noted that the maximum excess adsorption may fall to a higher pressure range up to 15 MPa. Hence, increasing the methane storage capacity at 3.5 MPa is not limited and the plateau region in the adsorption isotherm is not reached. This may result, for example, in underestimation of the potential of new types of porous structures and materials they form.

Further, in conformity with the purpose of this review, we will proceed to discussion of the available experimental results on the synthesis and technology of porous carbon materials for methane storage and the issues related to optimization of the porous structures of promising materials using various theoretical approaches.

3. Microporous carbon adsorbents

It has been noted above that microporous carbon adsorbents possess a number of unique physicochemical properties, which are useful for their efficient application in ANG systems. Owing to the choice of raw materials and process conditions for pore formation (activation), it is possible to fabricate an adsorbent that will have optimal morphology, porosity and chemical state of the surface for solving particular problems.

Microporous carbon adsorbents, or activated carbons,[65] are obtained from a variety of organic raw materials of plant origin (corn grains,[66] sorghum and wheat grains,[67] corn cobs,[68] coconut and other nut shells,[69] palm bark [70]); solid fossil fuels of different degrees of metamorphism (peat, petroleum coke,[71] brown and hard coals,[72] anthracite [73–75]); wood-based materials (wood, charcoal, sawdust, pulp and paper production wastes);[67,72] polymers,[8] as well as metal and non-metal carbides.[34,76,77] Carbon adsorbents manufactured from polymers, metal and non-metal carbides and nut shells possess high mechanical strength.

There are also other, exotic, sorts of raw materials for the synthesis of adsorbents, for example, wastes of agricultural rice production (activation with potassium hydroxide and orthophosphoric acid),[78,79] Aegle marmelos fruit (orthophosphoric acid activation),[80] seeds of tamarind, a leguminous tree,[81] agar-agar [82] and cellulose (physical activation by carbon dioxide).[9,83]

The industrial carbon adsorbents have specific features determined by the character of their surface and structure porosity. The carbon surface is electrically neutral, and adsorption on carbons is mainly due to dispersion interactions. The porous structure of carbon includes pores of all sizes, with the adsorption capacity and the rates of adsorption of components of industrial gases being determined by the content of micropores in unit mass or volume of the pellets. During adsorption, the micropores are volume-filled with the adsorbate.

Distinctive features of all carbon adsorbents are hydrophobicity and flammability.[55] When water is adsorbed on coals, the dispersion forces between water molecules and carbon surface are very weak. The initial stage of water adsorption is the chemisorption-induced formation of stable oxygen-containing radicals that are hydrogen-bonded to the carbon atoms on the micropore surface. These radicals, which have been called surface oxides, function as adsorption sites that bind other water molecules trough hydrogen bonds. The number of adsorption sites sharply increases with increasing pressure and, finally, the whole adsorption volume of micropores is filled with water. The volume of water loaded into carbon at high relative pressure ($P/P_s = 0.9$, where P_s is the saturated vapour pressure) is close to the limiting adsorption volume of the micropores. Hence, the adsorption capacity of carbon towards water vapour is closely related to its microporosity. However, saturation of ACs with water is very slow: the equilibrium is established during several months. Therefore, in most industrial processes, the humidity of the environment has almost no influence on the gas uptake and storage, and often even promotes adsorption as a result of hydrogen bonding to water molecules.[84] Activated carbon is the only type of industrial adsorbents that is hydrophobic; this accounts for their wide use.

In terms of particle size and shape, activated carbons are classified into powdered, pelletized and monolithic. Carbons used for ANG systems are, most often, pellets or monoliths, which is due to lower amount of dust and, hence, higher fire and explosion safety of the adsorbent. The use of adsorbents of different sorts is caused by the necessity to reduce the gas phase volume in the adsorber for increasing the performance. Therefore, the packing density of the adsorbent is distinguished as a very important parameter for storage systems.

In industry, activated carbons obtained from organic raw materials are used most widely. This is attributable to simplicity and low cost of their synthesis, because wastes of other production processes serve as the feedstock in this case. A considerable advantage of ACs is their relatively low cost; therefore, it is difficult to find a branch of industry that does not use activated carbons. Indeed, they are widely employed in the chemical, food and metallurgical industries, gas industry, communal services, mining production and nuclear power engineering. However, there is no separate AC class specially meant for storage systems for methane important for engineering.

Carbon adsorbents usually have high packing density values; therefore, it is possible to attain high specific volumetric characteristics for gas storage. There is a possibility to additionally increase the packing density by adsorbent compaction; this does not cause considerable degradation of the porous structure or adsorption activity. Since physical adsorption is accompanied by heat evolution, which has an adverse effect on the adsorption, it is important that the adsorbent have good heat conductivity. In the case of ACs, the heat conductivity is high.[85]

The major drawback of ACs is their flammability. In air, oxidation of carbons starts at temperatures >520 K. However, fire accidents at carbon adsorption plants are also known at lower temperatures. In particular, it was found that hydrogen sulfide corrosion of the equipment gives pyrophoric iron compounds such as FeS and Fe_2S_3, which ignite at relatively low temperature (being located in the bed, they act as ignition sites for the whole carbon bulk). In order to decrease fire hazard, up to 5% silica gel is sometimes added to carbon, the resulting adsorbent being called silicarbon.

The results of numerous studies of ACs attest to good prospects of these materials for methane storage systems. Some AC brands manufactured on an industrial scale are applicable for modern ANG systems after minor modifica-

tion. Thus, development of the fundamental theoretical and engineering basis for the synthesis of a new class of adsorbents for ANG systems is a relevant task. For this purpose, it is necessary to optimize the set of fundamental processes including the choice of the raw material, synthesis and modification, which would provide high values for key characteristics of ANG systems such as specific pore volume, characteristic energy of adsorption, large specific surface area and narrow pore size distribution.

As noted above, the raw materials used to prepare ACs for ANG systems can be divided into the following major groups: plant, fossil and synthetic raw materials and metal and non-metal carbides. An important factor is the initial raw material morphology, which determines the properties of the obtained porous sample.[55]

Carbonaceous raw materials are activated by physical or chemical methods or their combinations. In recent years, combined methods have been used more actively, because they allow fine tuning of the pore shape and size, which determine the adsorption energetics. The major physical activation processes are steam activation and carbon dioxide activation in oxygen-free environment at high temperature, in which volatile carbon compounds are generated and carried away, and the porous structure is formed. Chemical activation is often performed using acids (H_3PO_4, H_2SO_4), bases (KOH, NaOH) or sulfur compounds (K_2S) with subsequent carbonization under argon or nitrogen at 873–1280 K. The preparation of a porous material is often followed by chemical surface modification by various elements, moulding or compaction, which improve the material performance.

The progress of food industry led to increasing amount of wastes that can be efficiently utilized after processing. This is evidenced by numerous studies devoted to the processing of plant raw materials such as coconut shell, seeds, fruit stones, agar-agar, palm bark and so on. We will consider in more detail the most important types of raw materials regarding their applicability for activated carbon production.

3.1. Carbons from plant raw materials

3.1.1. Plant raw materials: corn grains and cobs

Balathanigaimani *et al.*[66] produced chemically activated corn grain-based carbons using carboxymethyl cellulose as the binder. The best methane storage capacity (100 $m^3\ m^{-3}$) was found for the adsorbent sample designated as MR-1/2-CMC-5% at 3.5 MPa and 293 K. This adsorbent was obtained at the activating agent to raw material mass ratio (r) of 1 : 2, while the carboxymethyl cellulose binder concentration was 5%. The structure and energy characteristics of the MR-1/2-CMC-5% sample are presented, including surface area determined by the Brunauer–Emmett–Teller method, $a_s(BET) = 2147\ m^2\ g^{-1}$; micropore volumes determined by the Dubinin–Radushkevich equation using nitrogen and carbon dioxide adsorption isotherms, $W_0(N_2) = 0.762\ cm^3\ g^{-1}$ and $W_0(CO_2) = 0.508\ cm^3\ g^{-1}$; and the packing density $d = 0.42\ g\ cm^{-3}$. The temperature and pressure dependences of methane adsorption on this adsorbent are shown in Fig. 5. The gravimetric characteristics of adsorption of the MR-1/2-CMC-5% sample are moderate and are inferior to those of other adsorbents; however, owing to the high packing density, this material can store a methane amount sufficient for practical application. However, the deliverable capacity value of 150 $m^3\ m^{-3}$ still was not attained.[66]

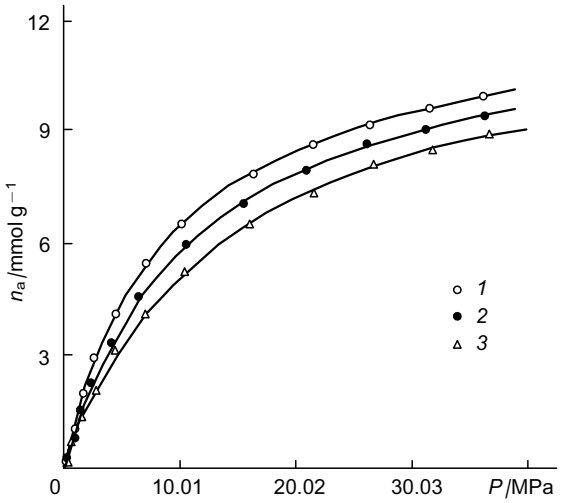


Figure 5. Adsorbed amount of methane on the adsorbent MR-1/2-CMC-5% *vs.* pressure at temperatures of 293.15 (*1*), 303.15 (*2*), 313.15 K (*3*).[66]

Corn cobs can also be used for the production of activated carbon.[68] The KOH activation was carried out at 823 K for 30–60 min. Samples with different degrees of activation at temperatures of 298.15 and 323.15 K were tested for methane storage. The two best samples had relatively high surface areas, $a_s(BET) = 1310$ and 1320 $m^2\ g^{-1}$, but moderate packing density of ~350 kg m^{-3}. This accounted, to some extent, for the relatively low maximum methane storage characteristics (Fig. 6). The methane adsorption at 3.5 MPa and 298 K was 120 $m^3\ m^{-3}$ (see the dot in curve *1*).

It was noted that the performance of the adsorption storage system based on these adsorbents can be increased by adjusting the optimal pressure in the system.[68] The variation of the volumetric specific capacity *vs.* pressure has a maximum in a strictly definite pressure range (see Fig. 6), in which the use of ANG systems with corn cob-based carbon adsorbents is most efficient. As the temperature increases, the total specific capacity of the system markedly decreases.

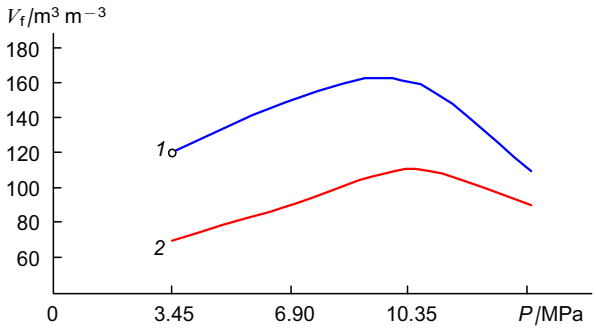


Figure 6. Volumetric specific capacity of the ANG system based on the sample with $a_s(BET) = 1320\ m^2\ g^{-1}$ *vs.* pressure at temperatures of 298.15 (*1*) and 323.15 K (*2*).[68]

For corn cob-based carbon [86] with the KOH : raw material ratio of 1 : 4 and carbonization temperature reaching 1123 K, the a_s(BET) value exceeded 3200 $m^2\ g^{-1}$. In addition, variation of methane adsorption by the obtained samples as a function of moisture content in the adsorbents was studied. As shown by analysis of the porous structure by X-ray diffraction, scanning electron microscopy and high-resolution transmission electron microscopy, the samples had a chaotic amorphous structure. Like other researchers, Liu *et al.* [86] noted a beneficial effect of wetting on the methane uptake, which is probably attributable to the formation of gas hydrates.

3.1.2. Plant raw materials: wheat and sorghum

Zhang *et al.*[67] studied carbon adsorbents produced from sorghum grains (average grain diameter of 3 to 4 mm, moisture content of 15%) and wheat grains (grain length of 6 mm, grain diameter of 2 mm, and moisture content of 8.4%). Carbonization was carried out at 573 K in a nitrogen atmosphere for 10–20 min. Chemical activation was carried out using aqueous solutions of orthophosphoric acid (35 mass %, 50 mass % and 85 mass %), zinc chloride (50%) or potassium hydroxide (50%) at 773–873 K. The obtained samples contained ~68% carbon, 18% oxygen and also sulfur, phosphorus, nitrogen and hydrogen impurities. The maximum specific capacity for methane was found for the sorghum-based activated carbon and amounted to 89 $m^3\ m^{-3}$, which approaches the value of 106 $m^3\ m^{-3}$ determined for commercial Calgon carbons. Activated carbon obtained from sorghum had a packing density of 0.65 $g\ cm^{-3}$, a_s(BET) = 2027 $m^2\ g^{-1}$ and W_0 = 0.76 $cm^3\ g^{-1}$.

Carbon samples were compacted to monoliths; the fractional composition of adsorbents was adjusted in order to obtain a high packing density. The authors noted high kinetic characteristics of the ACs, which was confirmed experimentally by direct measurement of desorption.[67] Methane adsorption was measured at 298 K and 3.5 MPa. The authors presented a linear dependence of the mass relative efficiency coefficient (the storage factor) (η_m) of the ANG system on the sample packing density as well as the dependence of η_m on the lignin content in the raw material (Fig. 7). The storage factor is defined as the ratio of methane mass adsorbed in the ANG system to the methane mass stored in the system without an adsorbent. In the authors' opinion, the optimal pore width was ~1 nm.

3.1.3. Plant raw materials: oil palm bark

Attempts have been made to synthesize ACs from oil palm bark.[70, 87, 88] In particular, the conditions of activation of ACs based on these raw materials (chemical activation with orthophosphoric acid and physical activation with carbon dioxide) were optimized.[70] The activation temperature and time and the degree of acid impregnation were chosen as the key process variables. The adsorbent performance was evaluated from the absolute methane adsorption.

The optimized surfaces derived from analysis of the adsorbed amount as a function of the activating agent : raw material ratio (r), temperature (T) and activation time (t) are presented in Fig. 8. It was found that the optimal conditions comprise the activation temperature of 1128 K, impregnation with H_3PO_4 at r = 9.42 : 1 and activation time of 135 min. The physicochemical activation led to a considerable increase in the methane adsorption, which reached 25.9 $cm^3\ g^{-1}$ at a pressure of up to 0.1 MPa and a temperature of 303 K. According to researchers' opinion,[70] the activation time is the most important of variables, because it determines the final degree of sample activation.

Carbon molecular sieves were also manufactured from oil palm bark [87] and studied for the adsorption and selectivity towards CH_4, CO_2, O_2 and N_2. The material was activated with K_2CO_3, and carbonization was carried out in a benzene flow with variation of temperature, time and benzene flow rate. The samples prepared at 1073 K and t = 20 min showed the highest methane adsorption capacity (the highest total specific capacity), which is accounted for by the greatest micropore volume (Fig. 9).

Niya *et al.*[88] investigated the sorption characteristics of the AC prepared from oil palm bark by chemical H_3PO_4 and $ZnCl_2$ activation followed by physical activation in a carbon dioxide flow. The goal of the study [88] was to elucidate the relationship between the adsorption activity and structure and energy characteristics of the samples. However, an unambiguous conclusion can hardly be drawn from the results, as the experiment was conducted at low pressure (up to 0.1 MPa). It is only worth noting that the most narrow pore size distribution is achieved for ANG

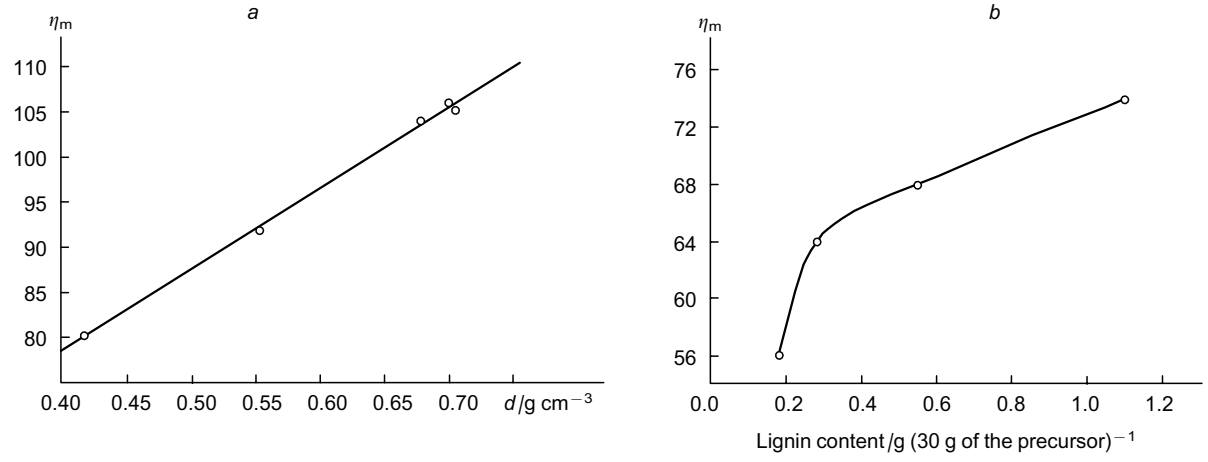


Figure 7. Dependences of the factor η_m on the adsorbent packing density (*a*) and lignin content in the raw material (*b*).[67]

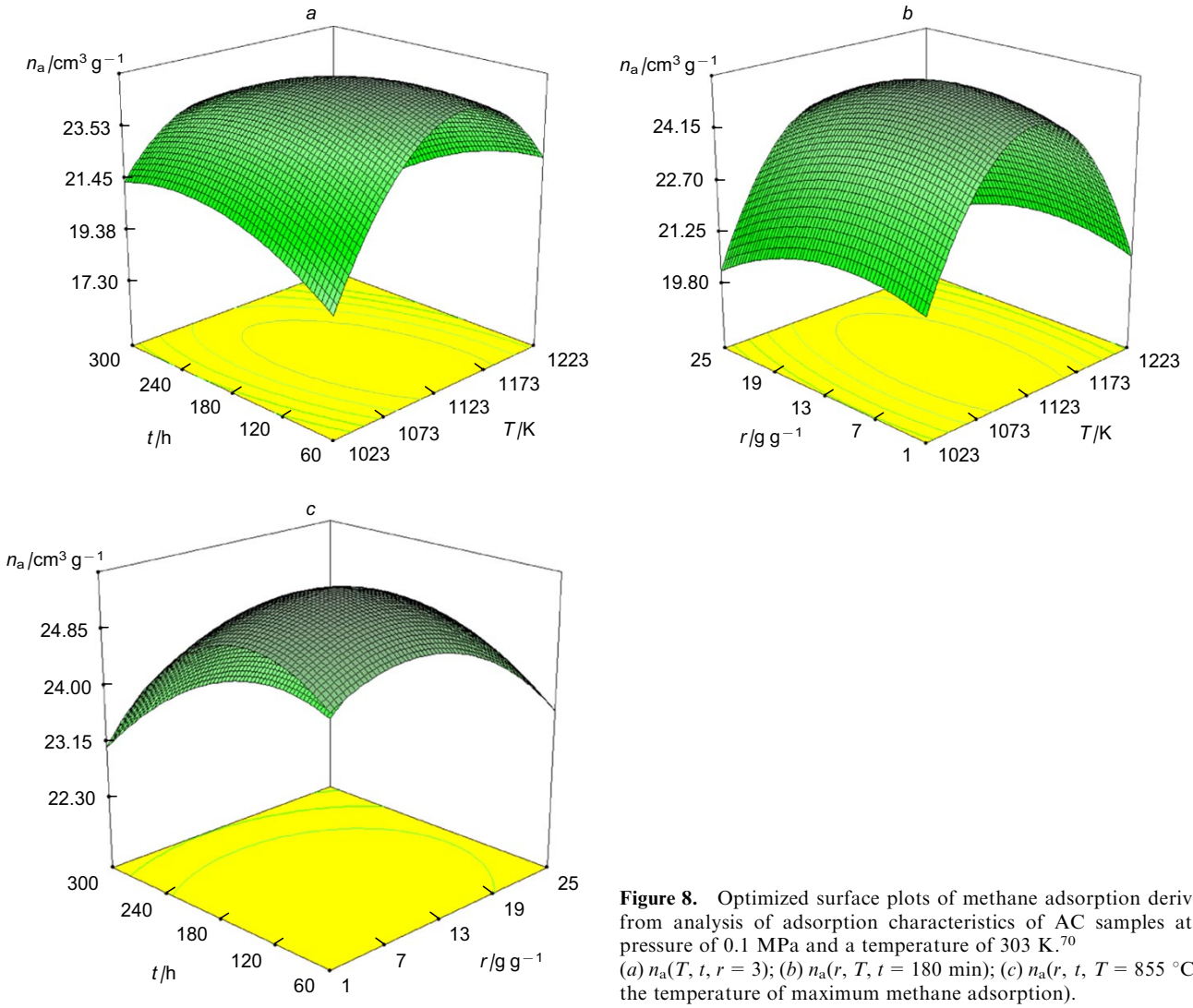


Figure 8. Optimized surface plots of methane adsorption derived from analysis of adsorption characteristics of AC samples at a pressure of 0.1 MPa and a temperature of 303 K.[70]
(*a*) $n_a(T, t, r = 3)$; (*b*) $n_a(r, T, t = 180$ min); (*c*) $n_a(r, t, T = 855$ °C is the temperature of maximum methane adsorption).

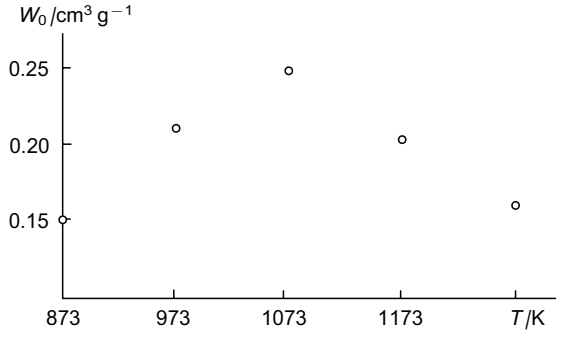


Figure 9. Correlation between the micropore volume of the oil palm bark-based adsorbent and activation temperature.[87]

system adsorbents when the samples are only chemically activated with moderate carbonization times.

3.1.4. Plant raw material: coconut shell

According to numerous studies, coconut shell is one of the most popular types of raw material used to produce activated carbons.[69,89–96] Coconut shell-based adsorbent samples have been prepared using physical steam activation, with the porous structure parameters of the samples varying depending on the degree of activation. The adsorption activities of samples with different moisture contents were investigated. According to Celzard and Mareche,[90] in the 0.81–1.05 g g^{-1} range of moisture ratios, the V_f value for the ACs reached 170–250 m^3 m^{-3}, whereas this value for a dry sample was 110–160 m^3 m^{-3}. The methane adsorption experiment was carried out at a temperature of 273 K and a pressure of up to 8 MPa.

Coconut shell-based carbons were chemically activated with zinc chloride or subjected to combined chemical and physical steam activation.[91] The combined protocol induces further development of the porosity (an increase in the micropore volume), with the energy characteristics being invariable, that is, the micropore shape and size virtually do not change, which appears important for the design of high-performance adsorption storage systems. The methane uptake of the resulting carbons was measured using a volumetric method at a pressure of up to 15 MPa.[91] Despite rather high W_0 values (> 1 cm^3 g^{-1}) and high methane uptakes of the sample, commensurable with these characteristics of laboratory and industrial samples (12 mass % at 298 K and 4 MPa), the V_f value did not exceed 80 m^3 m^{-3},

which was attributed to low packing density of the adsorbents.

Prauchner and Rodriguez-Reinoso[92] carried out physical activation with CO_2 and chemical activation with orthophosphoric acid and zinc chloride. It was noted that a combination of weak chemical activation and physical activation with carbon dioxide gives a structure with a narrow pore size distribution and insignificantly decreased packing density.[93] In order to maximize V_f, it is necessary to select and mix adsorbents of different particle size distributions. In this case, the optimal packing density can be attained.[92]

The dependences of methane storage on the porous structure parameters for monolithic samples of zinc chloride-activated carbon obtained from coconut shells have been investigated.[69] It was found that the textural parameters of the resulting carbons do not determine unambiguously their volumetric methane uptake. The surface properties (energy characteristics of adsorption) and equilibrium gas adsorption values (micropore volume) should be taken into account while choosing the adsorbent for methane storage.

In the case of the adsorbent AU-1,[53,97] the specific methane storage capacity at 300 K and 3.5 MPa was ~ 87 m^3 m^{-3} (Fig. 10 *a*), which corresponds to the results for other adsorbents based on plant raw materials, but is considerably lower than the required values.[29] However, the packing density of this adsorbent is very low (~ 380 kg m^{-3}); if the packing density is increased, for example, by forming a monolith, the adsorption capacity can be almost doubled.

As the storage system temperature decreases, the volume of stored methane increases. When the temperature decreases from the established 298 to 216 K, the adsorbent AU-1 can store ~ 150 m^3 m^{-3} of methane (see Fig. 10 *a*). The relative efficiency of methane storage in comparison with gas cylinder storage without an adsorbent reached ~ 2.5 for all studied temperatures at 3.5 MPa pressure (see Fig. 10 *b*). In other words, with other conditions being the same, the stored amount of methane is 2.5 times higher with AU-1 than without an adsorbent. It should be noted that for the adsorbent AUK, this ratio is ~ 5,[98] which is attributable to its packing density and surface heterogeneity.

3.1.5. Plant raw materials: cellulose

It has been shown[9] that microporous carbon adsorbents can be obtained from microcrystalline cellulose pellets. The authors used a cellulose powder with a crystal size of ~ 50 μm. About 1.5 g were placed into a press mould and the pressure was raised from 0 to 98 MPa, with the pressing time being varied from 1 to 60 min. The obtained pellets were carbonized in a furnace at a temperature of 1073 K in a nitrogen flow for variable periods of time (1 to 12 h) and then activated in a CO_2 flow at 1073–1173 K for 6 to 19 h. This gave AC samples with a specific surface area of up to 1700 m^2 g^{-1}. The highest methane storage capacity of the system with a HSAC sample was 147.2 m^3 m^{-3}.

The same authors[9] measured the durability of the adsorption capacity of the samples during cyclic operation (Fig. 11 *a*). A key feature of cyclic testing is reversibility of methane adsorption in the adsorbent. The adsorption–desorption cycles performed for the obtained AC samples simulated operation of real ANG systems. The tests revealed no decrease in the methane storage capacity.

It appeared of interest to find out how variation of the environmental temperature would affect the pressure change in a storage system (Fig. 11 *b*). The measurements were carried out at a 2 MPa pressure in the system and at room temperature. A closed storage system (maintained in the absence of heat exchange with the environment) was heated to 353 K. The most pronounced pressure change for the system with this adsorbent was $\sim$ 7%, while for a similar closed system without an adsorbent, this value was ~ 20%. Probably, this difference is caused by a smoother change in the properties of the adsorbent system with temperature rise in comparison with that in the gas phase; this rules out, for example, the rollover mentioned above and thus makes an additional contribution to the operating safety of ANG systems.

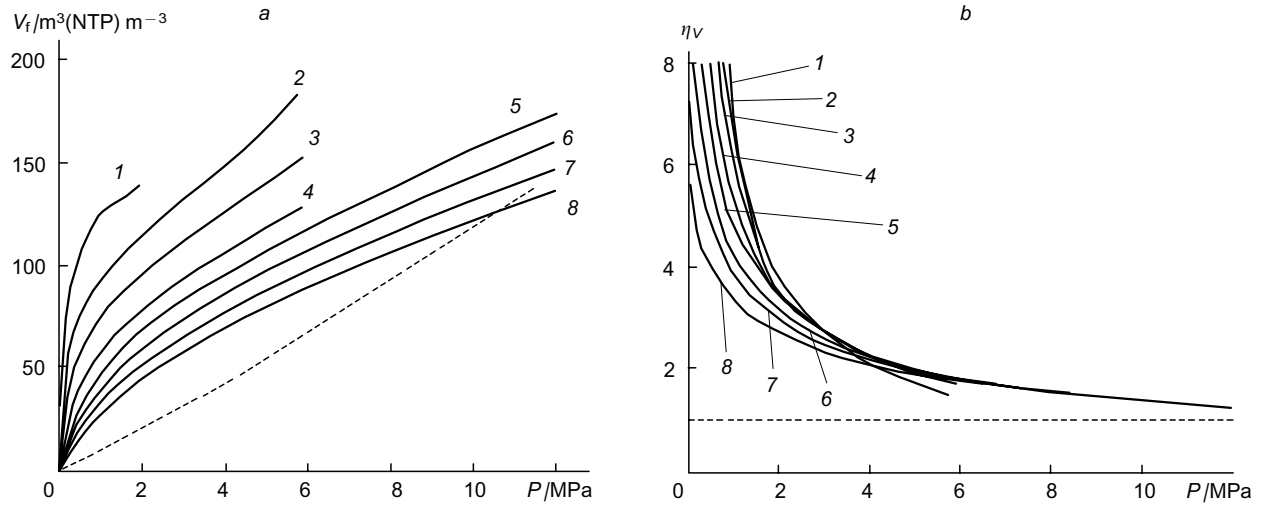


Figure 10. Total volumetric specific capacity for methane storage (*a*) and relative efficiency (*b*) of the microporous carbon adsorbent AU-1 *vs.* pressure at temperatures of 178 (*1*), 216 (*2*), 243 (*3*), 273 (*4*), 300 (*5*), 320 (*6*), 340 (*7*), 360 K (*8*).[53,97]
Dashed lines show the dependences for compressed gas storage at 293 K.

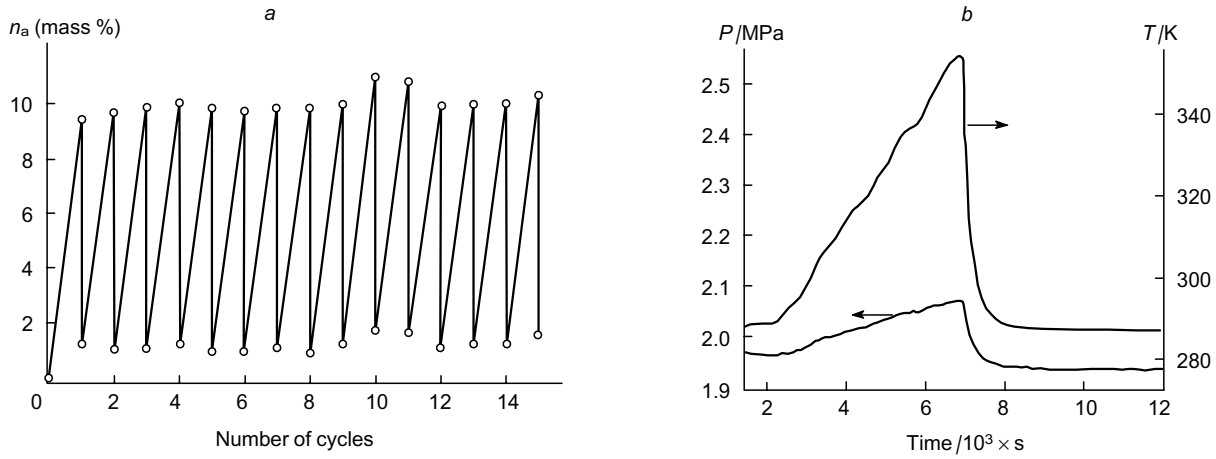


Figure 11. Variation of methane adsorption in an HSAC sample during sorption–desorption cycles (*a*) and methane storage pressure in a system with this sample with temperature rise (*b*).[9]

Synthesis of AC from lignin wastes of the pulp and paper industry has been reported.[99, 100] First, spherical resin particles were prepared by polycondensation of lignin sulfonates with cross-linking reagents, then the particles were carbonized in an argon atmosphere and activated with carbon dioxide, and finally the samples were moulded.[99] The highest V_d value for an ANG system with the resulting adsorbents was ~150 m^3 m^{-3} at 298 K and 3.4 MPa.[99]

3.1.6. Plant raw materials: olive stones, almond shells, peach stones and beans

Food industry wastes of production of olive oil and canned olives can be utilized for the manufacture of activated carbons.[101, 102] Djeridi *et al.*[101] reported the laboratory preparation of AC pellets from olive stones by chemical activation with orthophosphoric acid at temperatures from 623 to 1273 K and their adsorption characteristics at 303 K and up to 2.5 MPa pressure. The porous structure of the samples included micro- and mesopores, while the methane adsorption was relatively low: up to 5 mmol g^{-1} at 2.5 MPa. It is noteworthy that the highest adsorption was observed for samples activated at the boundary values of the activation temperature range. At these temperatures, the adsorbents had the largest micropore volumes (0.409–0.468 cm^3 g^{-1}) and BET surface areas.

The dependence of adsorption on the micropore volume is nearly linear (see the dashed line in Fig. 12). One of the conclusions drawn in the study is that not only the W_0 value, but also the pore size distribution must be taken into account while choosing the optimal sorbent. It was also noted that the micropore volumes determined from nitrogen adsorption data are not always trustworthy, as they do not take into account narrow pores that can adsorb methane.[101]

Djeridi *et al.*[102] analyzed the influence of the temperature of H3PO4 activation of an olive stone-based precursor on the micropore volume and size distribution. The sample with a greater pore volume and wider pores had a lower methane uptake than the adsorbent with smaller W_0, but with a pore size more appropriate for methane adsorption.

It was noted that ACs can be prepared from a mixed raw material based on olive and peach stones using a variety of chemical activating agents ($ZnCl_2$, KOH, H_3PO_4);[103] the effect of activation on the AC formation and on the properties of porous structure were studied. It was found that KOH activation is mainly accompanied by increasing proportion of micropores, $ZnCl_2$ provides the formation of mesopores, and H_3PO_4 promotes development of heterogeneous pore size distribution: micro-, meso- and macropores are formed. The highest volumetric specific capacity for methane storage (131 m^3 m^{-3}) was found for the sample with the highest content of micropores.

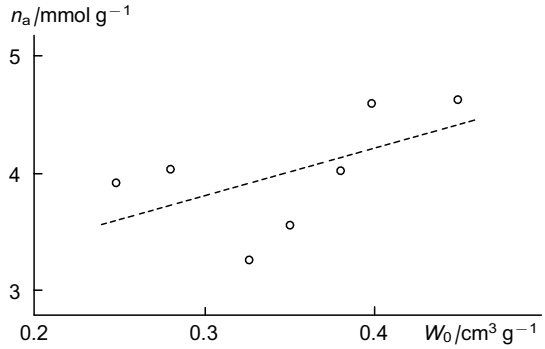


Figure 12. Correlation between the methane adsorption and micropore volume of carbon adsorbents activated at temperatures in the 683–1273 K range.[101]

The effect of structure and energy characteristics of adsorbents on the specific capacity of ANG systems was studied using laboratory AC samples prepared from various plant raw materials (olive and peach stones, almond shells and coconut shells) and also petroleum coke.[104] The porous structure parameters of activated carbons were found to depend substantially on the raw material. Three protocols were used to activate the raw materials:

— two-stage chemical activation of precursors without pretreatment;

— one-stage chemical activation of precursors after carbonization;

— upgraded two-stage chemical activation of precursors without pretreatment, which provides a packing density of at least 600 kg m^{-3}.

After activation, monoliths 4.5 cm in diameter were formed from all obtained AC powders. As a result, depend-

ing on the activation protocol, three samples were prepared from each type of precursor. The specific surface areas and volumes of micropores varied over rather narrow ranges, 2205–2515 $m^2\ g^{-1}$ and 0.982–1.374 $cm^3\ g^{-1}$, respectively, for all samples prepared from plant raw materials. The highest methane adsorption (215 mg g^{-1}) was found for the coconut shell sample activated according to the first protocol, while the greatest V_d value (184 $m^3\ m^{-3}$) was obtained for coconut shell and petroleum coke samples activated using the second protocol upon gas pressure drop from 6.89 and 6.95 MPa, respectively, to atmospheric pressure.

Comparison of the adsorption and capacity characteristics of the adsorbents and the pore size distribution showed that the optimal pore width for the activated carbons is ~1.5 nm.[104]

Worth mentioning are publications in which coffee husks and waste coffee grounds were used as raw materials to obtain activated carbons.[105, 106] Chemical activation was carried out [105] using orthophosphoric acid at $r = 1.5:1$ and zinc chloride and potassium hydroxide at various r values. The samples were pressed to form honeycomb monoliths using polyvinyl alcohol as a binder up to a maximum density of 0.6 g cm^{-3}. The highest V_f value was found to be 130 $m^3\ m^{-3}$ at 298 K and 3.5 MPa for the $ZnCl_2$-activated sample. The specific pore volumes of the samples varied from 0.59 to 0.84 $cm^3\ g^{-1}$, while the BET surface areas were from 890 to 1326 $m^2\ g^{-1}$.

Munusamy *et al.*[81] prepared ACs by chemical activation of tamarind seeds with potassium hydroxide. The optimal porous structure of the adsorbent for the use in ANG systems was adjusted by varying the activation parameters such as temperature, time and the precursor to activating agent mass ratio.

3.2. Carbons from polymer raw materials

3.2.1. Polymer raw materials: carbon fibres

Carbon fibres were prepared by electrospinning of a polyacrylonitrile solution in *N*,*N*-dimethylformamide.[8] The fibres were activated with K_2CO_3, the r ratio was 3:1 and 5:1; in the authors' opinion, this promoted the formation of a porous structure with an appropriate volume for methane adsorption. The fibres were activated at 1323 K under argon for 3 h. This was followed by fluorination of materials for surface modification to increase the methane adsorption energy. The samples were designated as F-EsACF-*i* (electrospun activated carbon fibres), where *i* stands for the activating agent : precursor molar ratio, F means surface fluorination. The carbon fibres were packed at pressures up to 1200 MPa to improve characteristics of stored methane.

The packed samples labelled as F-EsACF-5 and F-EsACF-3 had large BET specific surface areas, 2500 and 1600 $m^2\ g^{-1}$. The authors indicated that packing decreased only slightly the specific surface area (by not more than 5%). The average effective pore sizes of the obtained samples were in the range of 0.7–1.6 nm.

Fluorine modification of the carbon fibre surface substantially affected the stored methane volume. The functional groups formed on the carbon surface upon fluorination generate additional electrostatic interactions, due to the high electronegativity of fluorine, which markedly increases methane adsorption (Figs 13 and 14).

The synergistic effect caused by highly developed microporous structure and polarization of methane molecules by fluorine at the pore inlet (see Fig. 13) increases the methane

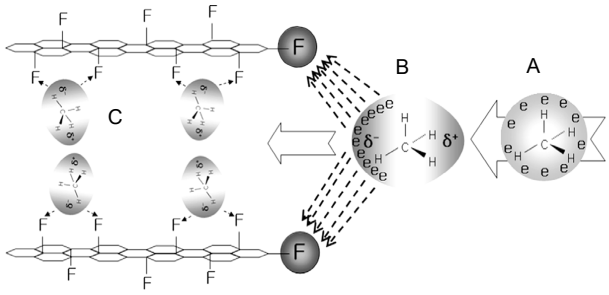


Figure 13. Schematic mechanism of adsorption of methane molecules in a model adsorbent with a fluorine-modified surface.[8]
A is a methane molecule; B is a polarized methane molecule; C is the molecule adsorbed in a pore.

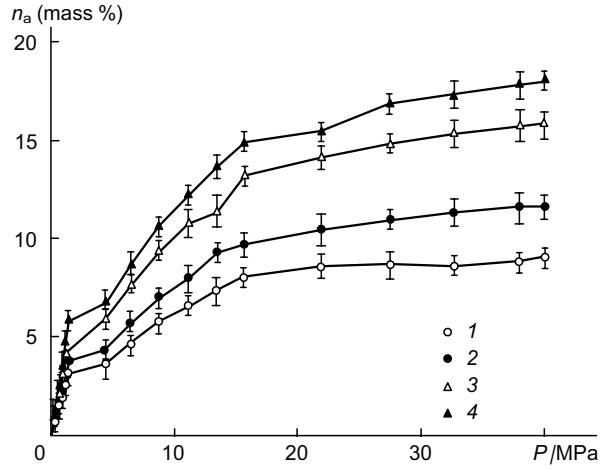


Figure 14. Methane adsorption for non-modified (*1*, *3*) and fluorine-modified (*2, 4*) samples of fibre-based activated carbons *vs.* pressure at a temperature of 298 K.[8]
Sample: (*1*) EsACF-3, (*2*) F-EsACF-3, (*3*) EsACF-5, (*4*) F-EsACF-5.

uptake up to 18.1 mass % (see Fig. 14), which corresponds to a capacity of 191.3 $m^3\ m^{-3}$.

3.2.2. Polymer raw materials: phenolic resins

The synthesis and adsorption characteristics of activated carbons based on phenolic resins are analyzed in a number of publications.[30, 78, 107] The adsorption of methane in monolithic samples formed from phenolic resins using variable conditions of physical activation with carbon dioxide was studied by a volumetric method.[30] It was found that excessive activation of the precursor up to high specific surface areas and volumes of micropores has an adverse effect on the storage capacity of materials due to a sharply decreasing packing density. Measurements of the cyclic stability of the samples and their adsorption–desorption characteristics showed that AC samples can store up to 150 $m^3\ m^{-3}$ of methane at 298 K and 3.5 MPa.[30]

Phenol formaldehyde resin was also proposed for the synthesis of carbon materials [107] meant for methane storage. The differential molar isosteric adsorption heats (q_{st}) were found to reach 25 kJ mol^{-1}, which attests to high energy characteristics of these samples; the effective pore width

exceeded 2 nm. The methane adsorption was measured with variable temperature and pressure in the ranges of 298 to 318 K and 1 to 4 MPa, respectively. At 3.5 MPa and 298 K, adsorption reached 9 mmol g^{-1}, which attests to good prospects of this type of AC for methane storage.

Ben *et al.*[108] succeeded in the preparation of an AC with a bimodal pore size distribution from a KOH-activated carbonized porous aromatic structure. According to measurements, the pore sizes in the sample were 0.6–0.8 nm and >1.2 nm. This should ensure high methane uptake over a broad pressure range. Indeed, it was found that the adsorption characteristics are better for this sample than for the adsorbents with a uniform porous structure at both low and high pressures.[108] The methane adsorption reached 12.5 mmol g^{-1} at 3.5 MPa and 298 K, which opens up certain opportunities for using this material for methane storage.

3.2.3. Polymer raw materials: organosilicon polymers and furfural polymer

Activated carbons have been prepared from two types of polysilsesquioxane with the empirical formula $(RSiO_{1.5})_n$, where R = Me (polymethylsilsesquioxane) and R = Me–Ph (polymethylphenylsilsesquioxane).[109] Pyrolysis was carried out at 1473 K for 2 h until various SiOC ceramics were formed. Then ceramic samples were etched in a chlorine flow at 1473 K. The a_s(BET) values, the total pore space (W_t) and the average effective micropore widths (X_0) are presented below:

Sample	a_s(BET) /m^2 g^{-1}	W_t /cm^3 g^{-1}	X_0 /nm
SiOC-CDC-1	2593	1.403	2.0
SiOC-CDC-2	2364	1.72	2.6

This approach to the synthesis of carbon adsorbents resulted in excess methane uptake of 18.3 mass % and 14.2 mass % for SiOC-CDC-1 and SiOC-CDC-2 samples, respectively.

Fomkin *et al.*[110] studied the microporous carbon adsorbent FAS-VA (Ref. 111), which was obtained from furfural-based polymer raw material. High-strength adsorbent pellets were formed as spheres 0.5–2 mm in diameter. According to the technical specification,[112] the spherical pellets of the sorbent are formed upon liquid moulding of the furfural and epoxy resin copolymer, which comprises stages of monomer resinification, forming of spherical pellets from the mixture and curing of the pellets. The spherical pellets are activated in a thermochemical reactor with a steam and carbon dioxide mixture at temperatures up to 1173 K. The packing density of the adsorbent is 0.300 g cm^{-3}. It was found[110] that the FAS-VA material has a bimodal microporosity; therefore, the methane adsorption increases, especially at high pressure. An advantage of ANG systems based on FAS-VA over CNG systems was established for broad ranges of pressures (5 to 12 MPa) and temperatures (273 to 333 K); the V_f value approached 200 m^3 m^{-3}. A characteristic maximum was detected in the $q_{st}(n_a)$ plot in the region of medium degrees of filling, which attests to the formation of associates of adsorbed molecules. The authors[110] noted that adsorption can be enhanced by using structures in which the adsorption energy is increased due to association of adsorbate molecules in micropores.

3.3. Carbide-based carbons

Carbides are high-melting, refractory and chemically inert solids. In recent years, synthesis of carbon adsorbents from carbides has been receiving a lot of attention, because this may give high-quality systems with uniform microporosity. Ordered structures can be generated in the porous carbon matrix upon removal of metal and non-metal atoms from a carbide. Most often, silicon, titanium and calcium carbides are used for this purpose.[98, 109, 112–115]

The adsorbent AUK was obtained by thermochemical leaching out of silicon atoms from silicon carbide[98] at 1173 K. The formation of the adsorbent proceeds according to the equation

$$SiC + 2Cl_2 \longrightarrow SiCl_4 + C \quad (8)$$

The resulting carbon template has high hardness and extensive pore volume. The adsorbent possesses high surface heterogeneity and can be prepared in the monolithic form; hence, the packing density can be high. This determines its excellent performance for methane storage (Fig. 15).

At a temperature of 293 K and a pressure of 3.5 MPa, the adsorbent AUK is able to store about 160 m^3 m^{-3} of methane, which complies with the DOE requirement of 1997.[29] When the temperature slightly decreases from the established 298 to 273 K, AUK can store up to 190 m^3 m^{-3} of methane, which corresponds to the volumetric capacity required by the DOE in 2000.[30] A temperature decrease by 82 K (down to 216 K) will bring the methane volume stored by an AUK-based system to the level of DOE requirements of 2012.[35] Thus, the requirement to the volume of stored methane can be met by decreasing temperature of the storage system; however, operation of these systems is associated with certain energy expenditures and difficulties.

Li *et al.*[113] also described the results of a comprehensive study of ACs based on silicon carbide; the authors determined key parameters (crystalline density of pellets, packing density, BET surface area) for samples synthesized under

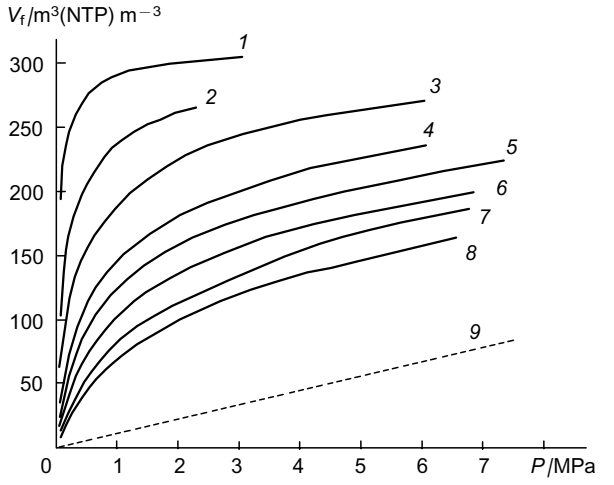


Figure 15. Specific volume of methane stored by the microporous carbon adsorbent AUK *vs.* pressure at temperatures of 178 (*1*), 216 (*2*), 243 (*3*), 273.15 (*4*), 293 (*5*), 313 (*6*), 333 (*7*), 353 (*8*); (*9*) compressed gas at 293 K.[98]

various conditions. In the authors' opinion, high specific capacity, which reaches 145 $m^3\ m^{-3}$ at 3.5 MPa and 298 K, is due to high packing density of the adsorbent.

Krockrick *et al.*[114] described the synthesis of mesoporous AC samples as tubes and rods from SiC particles and the results of measurements of methane, n-butane and hydrogen adsorption in these ACs. The adsorbent formed upon removal of silicon atoms in a chlorine flow at 1273 K and subsequent treatment in a hydrogen flow had good adsorption properties $n_a = 0.208\ g\ g^{-1}$ at 10 MPa and 298 K. The structure and energy characteristics of the samples were shown to surpass those of existing analogues.

Yeon *et al.*[77] carried out comprehensive analysis of methane adsorption in the ACs obtained from titanium carbide by removal of the titanium atoms in a chlorine flow and subsequent chemical (potassium hydroxide) or physical (carbon dioxide) activation under variable conditions. The data on methane adsorption were obtained experimentally on a volumetric setup at pressures of up to 6 MPa and a temperature of 298 K for samples with $a_s(BET) = 1113–3360\ m^2\ g^{-1}$, $W_0 = 0.5–1.36\ cm^3\ g^{-1}$. The maximum adsorption at 298 K and 3.5 MPa was found for the sample obtained by physical activation with CO_2 at 1148 K for 8 h, although this sample did not possess the maximum $a_s(BET)$ and W_0 values, and the calculated V_f value was $\sim 240\ m^3\ m^{-3}$. At higher pressure, the adsorption capacity was maximum for the samples with higher specific pore volumes and surface areas. The authors noted that the capacity of 240 $m^3\ m^{-3}$ was determined for the crystalline rather than packing density of the adsorbent. Analysis of the low-temperature methane adsorption demonstrated that by decreasing the temperature by 25 K from the 298 K level, one can increase the volumetric density of the stored methane by ~30%.

High characteristics of methane adsorption were reported for AC samples based on silicon oxycarbide.[109] At 6 MPa and 298 K, excess adsorption was determined to be 13.5 mmol g^{-1} (or 21 mass %), which is a high value.

3.4. Templated carbons

Guan *et al.*[116] used the template synthesis technique to prepare an AC sample. The ammonium form of type Y zeolite ($SiO_2 : Al_2O_3 = 5.1$) was used as the template; it was impregnated with poly(furfuryl alcohol), then pyrolyzed for 4 h at 1323 K in a nitrogen flow and etched with an acid to remove the template. The resulting sample labelled as C1050 was a finely dispersed powder with a high BET specific surface area (2135 $m^2\ g^{-1}$) and relatively large micropore volume (0.76 $cm^3\ g^{-1}$), but a low bulk density (0.28 $g\ cm^{-3}$) and, as a consequence, low volumetric density of the stored methane (60 $m^3\ m^{-3}$). In order to increase the packing density, the powder was pelletized; for this purpose, a 400 mg sample was sealed into an aluminium foil container. The resulting system was hot-pressed at 473 K and 50 MPa for 4 h. Then the system with the compressed sample labelled as C1050P (P means pelletized) was cooled in air. During hot pressing, the sample has lost some of the porous space [$a_s(BET) = 932\ m^2\ g^{-1}$, $W_0 = 0.4\ cm^3\ g^{-1}$], but the packing density considerably increased (up to 0.98 $g\ cm^{-3}$), as well as the volumetric capacity for methane (up to 127 $m^3\ m^{-3}$).

Activated carbons with a narrow pore size distribution can be obtained by impregnation of a carbon-containing compound into an ordered template, which is then removed. For example, ZTC structures are synthesized in this way, with a zeolite acting as the template. Stadie *et al.*[117] used the volumetric method to study the adsorption and thermodynamic properties of some ACs such as CNS, MSC and ZTC at temperatures from 238 to 526 K and at a pressure of 10 MPa (Fig. 16). Note the increase in the isosteric heat of methane adsorption in the sample ZTC-3 caused by the contribution of intermolecular interactions between methane molecules at high coverages and by the formation of associates of adsorbed molecules. For other two samples (CNS-201 and MSC-30), the isosteric heats of adsorption decrease with increasing uptake over the whole range of coverages (θ); however, in the case of ZTC-3, the q_{st} value increases for $\theta = 0–0.6$. Presumably, this feature would be beneficial for ANG systems, as the differential isosteric heat of adsorption is maximum in the high pressure region; hence, less gas will remain in the system after delivery.

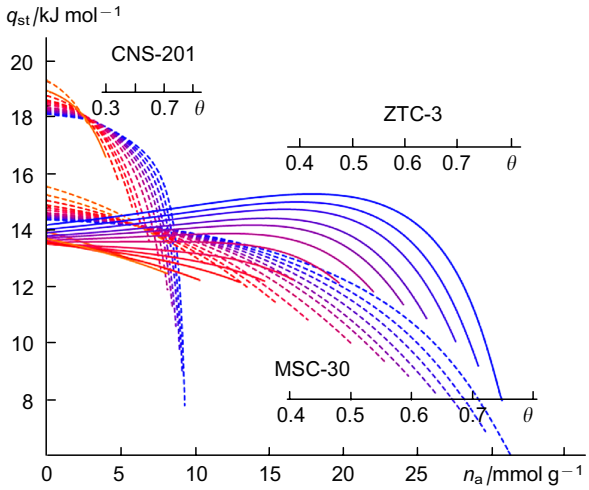


Figure 16. Isosteric heat of methane adsorption on carbon adsorbent samples *vs.* uptake in the temperature range from 238 to 523 K [the temperature is indicated by the colour of curves from blue (238 K) to red (523 K)] for the samples CNS-201, MSC-30 and ZTC-3.
The scale bars for each carbon adsorbent mean the coverage θ.[117]

Zeolite-like carbon structures were synthesized by chemical deposition of acetylene on the β-zeolite 930NHA in the 1023–1123 K temperature range in an argon flow followed by washing in 10% HF.[118] Methane adsorption measurements showed that, despite the highly ordered structure and a relatively large micropore volume (up to 0.75 $cm^3\ g^{-1}$), the ACs had low q_{st} and n_a values (at 3.5 MPa and 298 K): up to 13 kJ mol^{-1} and 5 mmol g^{-1}, respectively.

It is noteworthy that the vast majority of works dealing with the synthesis of new and investigation of existing carbon adsorbents for methane storage consider adsorption only at 298 K. However, it is obvious that by decreasing the temperature of a storage system, it is possible to markedly increase the stored gas volume. A number of publications[53, 97, 98, 119] report comprehensive studies of the adsorption in microporous carbon adsorbents based on silicon carbide[98] and various sorts of organic raw materials[53, 97, 118] at temperatures from 178 to 360 K and pressures up to 20 MPa.

3.5. Carbon adsorbents based on fossil fuels, petroleum products and peat

Natural coal is one of the most abundant types of fossil resources, which is demanded in power generation, metallurgy and other industries. A current trend is application of coal as the raw material for the manufacture of efficient adsorbents. Today, active carbons based on fossil coal account for a considerable part of carbon adsorbents.[120] Anthracite is a highly metamorphic ancient fossil coal; it is rich in carbon and has a graphite-like structure. The use of anthracite as a raw material for the production of ACs reduces the energy expenditure for the primary carbonization and ensures the formation of an ordered porous material owing to the minimum number of defects in the carbon crystal lattice. Thus, the synthesis of ACs from anthracite and natural coals is an important area of the design of ANG systems.

A number of publications[38, 73, 121] address the adsorption of methane in AC samples based on anthracite chemically preactivated with KOH taken in different ratios to the precursor and the effect of the activation conditions on the structure and energy characteristics and methane specific adsorption properties. The samples synthesized by Lozano-Castello *et al.*[73] had high BET specific surface areas (up to 3500 $m^2\ g^{-1}$) and large volumes (up to 1.53 $cm^3\ g^{-1}$) of micropores. It was found that the conventional evaluation of the adsorbent activity by analysis of the pore surface area and volume is not always valid, while the pore size distribution is the most important porosity characteristic. Lower values for specific adsorption of methane were found for samples with large micropore volumes than for other adsorbents. This was attributed to pore size distribution details. It was found that an increase in the activating agent : precursor mass ratio results in increasing BET specific surface area and increasing number of mesopores in the adsorbent, which decreases the methane adsorption. Simultaneously, the crystalline density of AC samples increases due to the decrease in the proportion of amorphous carbon.[73, 122]

The effect of variation of the pyrolysis temperature from 973 to 1223 K on the methane uptake of AC samples was analyzed.[73] Higher pyrolysis temperature resulted in a wider pore size distribution and lower proportion of ultramicropores and thus decreased the uptake. According to experiments, the time of pyrolysis had a slight effect on the methane uptake of the samples. The following activation conditions were recognized as optimal: $r = 3:1$, $T = 1023$ K, $t = 2$ h. Additionally it was found that the calculated V_f values for ANG systems with the obtained samples were lower than experimental values. Lozano-Castello *et al.*[38] also produced monolithic samples. The following types of binders were used: poly(vinyl alcohol), sodium salts of humic acids, phenolic resin, Teflon, cellulose binder and a WSC binder (the abbreviation stands for the manufacturer, Waterlink Sutcliffe Carbons).

Perrin *et al.*[122] considered the effect of NaOH activation temperature on the structure and energy characteristics and methane storage performance of anthracite-based activated carbons. The pressure dependences of methane density in micropores of different width were plotted. The highest density of the adsorbed phase was attained for the effective pore width of ~0.8 nm. The methane adsorption equilibria were obtained separately for the whole pore space and for micropores. It was found that the proportion of super-

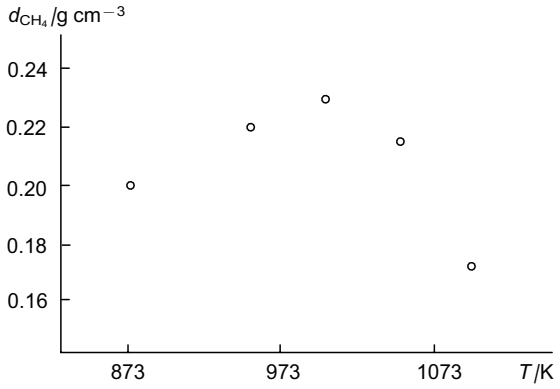


Figure 17. Correlation between the adsorbed methane density in the AC sample prepared from anthracite and the raw material activation temperature.[122]

micro- and mesopores increases with increasing activation temperature, which is in line with the results of other publications. The maximum in the pore size distribution curve shifts to wider pores; the curve for the density of adsorbed methane *vs.* activation temperature also passes through a maximum (Fig. 17). The dependences of storage capacity on a_s(BET) and on the micropore volume found from the nitrogen adsorption isotherm were elucidated. They were found to be descending and nearly linear. It follows from Fig. 17 that the highest methane density is found in adsorbents that were activated in the temperature range of 973–1023 K.

In a study of methane adsorption in ACs prepared from fossil coal and chemically activated with potassium sulfide at 298 K and up to 5 MPa, the dependence of n_a on a_s(BET) was found as an increasing linear function.[72] However, it must be noted that the study involved only low a_s(BET) values ranging from 5 to 700 $m^2\ g^{-1}$, which is insufficient for full characterization of ANG systems. Zhang *et al.*[71] reported data on AC synthesis from coke chemically activated with potassium hydroxide. The optimal activation conditions that provide the highest uptake and volumetric deliverable capacity of methane were determined to be as follows: the temperature range from 1073 to 1123 K and pyrolysis time of ~1 h.

Approaches to AC preparation from anthracite with NaOH chemical activation have been formulated.[100] The activation characteristics that should be optimized include temperature, activating agent : precursor mass ratio and the post-treatment conditions. The activation conditions resulting in the highest V_f value are as follows: $T = 953–973$ K and $r = (2.5–3):1$.

The synthesis of activated carbons and studies of their methane adsorption performance have been analyzed.[123] A distinctive point of this publication is optimization of the conditions of thermochemical synthesis of ACs from a decanted oil emulsion and ethylene tar pitch using KOH as the activating agent to form the optimal porous structure and minimize the loss of packing density. The optimal parameters of the synthesis, resulting in the formation of a monomicroporous adsorbent structure without mesopores, but with maintained kinetic characteristics are the following: $r = 3:1$, $T = 973$ K. The AC samples obtained under optimal conditions had a capacity of $>150\ m^3\ m^{-3}$ at

298 K and 3.5 MPa. Meanwhile, it was noted that the use of adsorbents in the pressure range from 5 to 10 MPa requires a certain proportion of narrow supermicropores (~1–2 nm). Thus, adsorbents with a definite pore size distribution should be selected for particular operating conditions of ANG systems.

Shkolin *et al.*[124] investigated the adsorption behaviour of the microporous carbon adsorbent AU-4 obtained from peat and subjected to potassium sulfide activation in order to evaluate the methane storage efficiency in the temperature range of 178–360 K and a pressure of up to 25 MPa. The highest amount of methane stored in these pressure and temperature ranges was found to be 160 $m^3\ m^{-3}$. Efficient methane storage in AU-4 over the whole temperature range is possible only for pressures from 1 to 7 MPa; at room temperature, the highest effect can be attained at pressures of 3–7 MPa.

3.6. Carbon adsorbents from miscellaneous types of raw materials

Exotic types of raw materials have been used for the synthesis of carbon adsorbents for methane storage systems. Attempts have been made to obtain ACs using crab shells and wastes of the shochu beverage production.[125] The synthesis processes and sorption characteristics of relatively new types of materials, carbon cryo- and aerogels, have been analyzed.[126] On the basis of published data, an optimization mathematical model was developed [127] for determination of the required conditions of carbon adsorbent synthesis depending on the specified level of specific storage capacity.

However, the storage capacity achieved for these ACs so far does not make them suitable for application in methane storage systems.

3.7. Composite materials based on carbon adsorbents

The use of MOFs in ANG systems is limited by their shortcomings: instability, hydrophilicity and susceptibility of porous structure to degradation. However, there is a possibility of efficient use of composite materials comprising MOFs and, for example, carbon adsorbents. Kayal and Chakraborty [128] described the synthesis of a composite material using the high-performance carbon adsorbent Maxsorb-III and metal-organic frameworks based on chromium(III) complexes, MIL-101(Cr), and studied the structure and energy characteristics and morphology as well as methane adsorption performance of the composite. Note that the AC was considered as an additional binding agent (~1 mass %) and MOF was the functional material.

In the first stage of composite synthesis, a mixture of 4 g of $Cr(NO_3)_3 \cdot 9H_2O$, 1.66 g of $HO_2C-C_6H_4-CO_2H$, 50 mg of Maxsorb-III, 1 ml of HCl and 50 ml of H_2O was prepared. This mixture was placed into an autoclave and then into an oven in which it was kept for 12 h at 473 K, and after that the autoclave with the precursor was cooled down to room temperature. Then dimethylformamide was added to the precursor and the mixture was heated to 353 K in order to remove the unreacted terephthalic acid from the pores. The product was activated in ethanol at 353 K for 12 h, separated and dried.

The adsorption properties of the composite were intermediate between those of the initial AC and MOF (Fig. 18 *a*); the situation changes slightly for the specific capacity: the ANG system with MAX-MIL demonstrates the highest value of V_f (Fig. 18 *b*). The authors [128] noticed improved operation properties of the composite, in particular, somewhat increased hydrophobicity of the resulting material in comparison with the initial MOF. Thus, the considered synthetic technology can be promising for the possible application of MOFs in ANG systems.

3.8. Effect of impurities on the methane adsorption

The impurity components such as heavy hydrocarbons, water, CO_2 and N_2 influence the methane adsorption, in particular during cyclic operation. Rios *et al.*[129] used the pelletized commercial activated carbon WV manufactured by Mead Westvaco (US) as the adsorbent.

The adsorption of methane as a natural gas component is 10%–15% lower than the adsorption of pure methane (Fig. 19 *a*). This is due to competitive adsorption of all

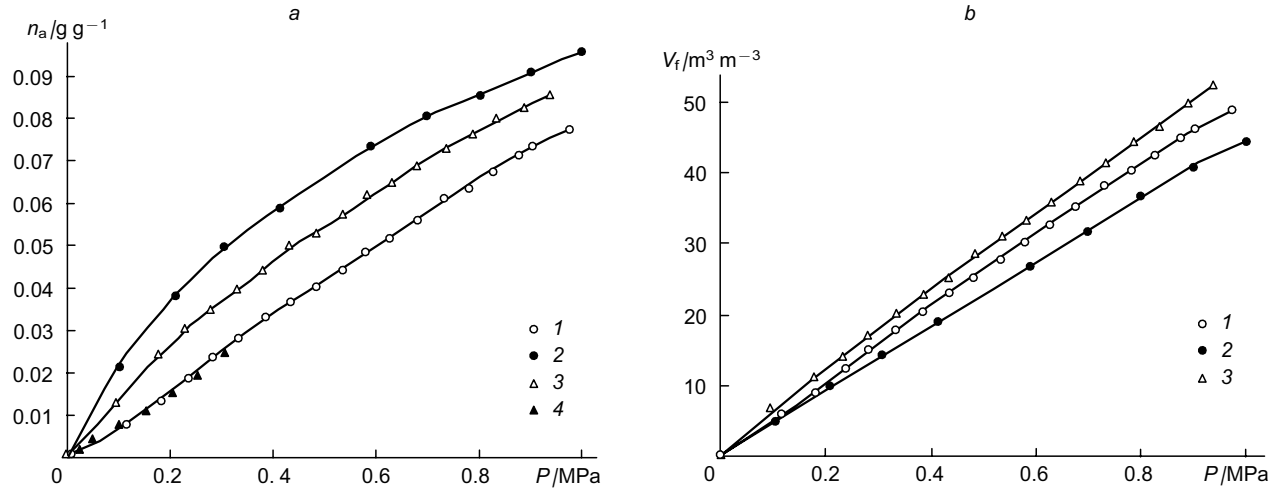


Figure 18. Pressure dependences of gravimetric methane adsorption (*a*) and total volumetric specific capacity (*b*) of an ANG system based on various carbon adsorbents at 300 K.[128]
Adsorbent: (*1*) MIL-101 (Cr), (*2*) Maxsorb-III, (*3*) MAX-MIL, (*4*) MIL-101(Cr) (see Ref. 40 in Ref. 128).

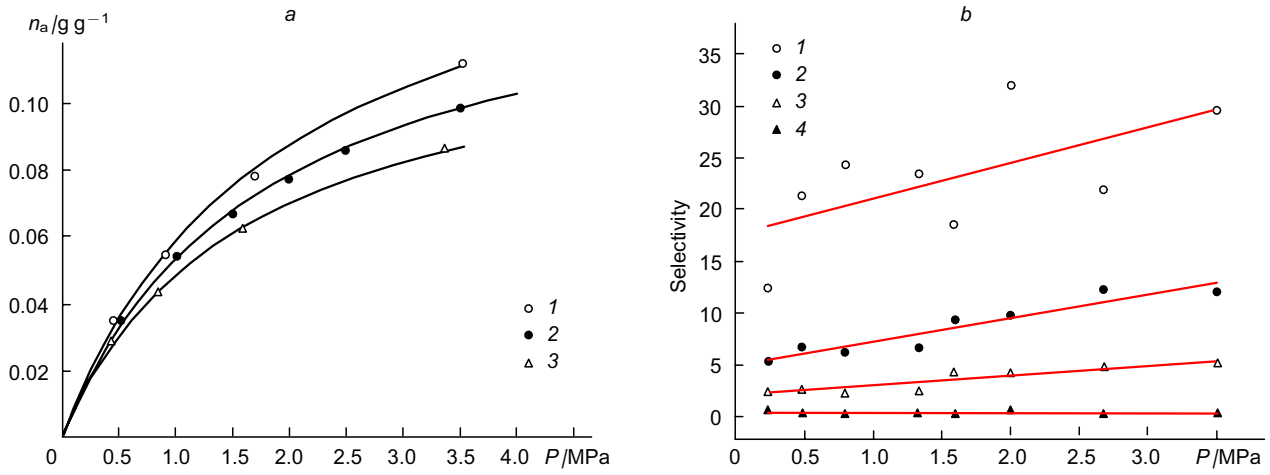


Figure 19. Adsorption isotherms of methane, natural gas, and methane from natural gas on the activated carbon WV1050 at 298 K (*a*) and adsorption selectivities to ethane, propane, carbon dioxide and nitrogen relative to methane at 298 K (*b*).[129]
(*a*) (*1*) Natural gas, (*2*) pure methane, (*3*) methane from natural gas; continuous lines correspond to calculation by the Langmuir equation; (*b*) (*1*) propane, (*2*) ethane, (*3*) carbon dioxide, (*4*) nitrogen; the lines correspond to approximation and the dots are experimental data.

natural gas components. Among the gas mixture components, only nitrogen adsorption is energetically unfavourable (Fig. 19 *b*); therefore, N_2 remains in the gas phase. Carbon dioxide, ethane and propane are sorbed much better than methane, with their relative selectivities increasing with a rise of pressure. This should be taken into account in the design of methane storage systems, because adsorption capacity may decrease during charge–discharge cycles due to accumulation of these mixture components. The results of analogous studies can also be found in other publications.[130, 131]

3.9. Cyclic operation of the adsorption storage systems

The volume of methane delivered from a storage system is, most often, markedly lower than the stored volume, because pressure in the system decreases from high to atmospheric, and a part of methane and other natural gas components remains in the adsorbent. Rios *et al.*[129] analyzed this behaviour of the system (Fig. 20). It can be seen that ~20% of the adsorption capacity is lost in the first six charge–discharge cycles and, after that, the n_a value barely depends on the number of cycles. The deliverable specific capacity of a methane storage system virtually does not change during cyclic operation; therefore this value is more useful for evaluation of storage system performance.

It is worth noting that the results are consistent with the data of other studies (see, for example, Refs 130 and 132).

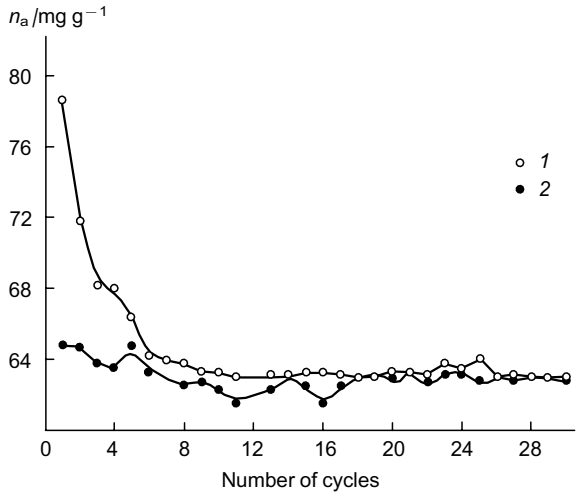


Figure 20. Total specific capacity (*1*) and deliverable capacity (*2*) for natural gas of a storage system *vs.* the number of charge–discharge cycles at 298 K and pressures of 3.5 (*1*) and 0.1 MPa (*2*).[129]

4. Increase in the efficiency of adsorption methane storage systems based on carbon adsorbents

4.1. Increase in the packing density of carbon adsorbents

The key parameters of the performance of an adsorption storage system are V_f and V_d. The gas density in the adsorption force field within the pores is much higher than the density of the free gas phase. Evidently, for equal thermodynamic conditions, the smaller the space free from the adsorbent in the ANG system, the greater the gas density converted to the actual system volume. Thus, the adsorbent packing density is a key characteristic. The following types of density are distinguished: the adsorbent skeletal density, or crystalline density (d_{cr}), density of an adsorbent pellet of monolith called apparent density (d_{ap}) and packing density (d). The last-mentioned value determines V_f and V_d of ANG systems. Thus, the packing density is a key characteristic for the performance of the adsorption storage system. This value is determined by the following factors:

— raw material type and content of impurities (*e.g.*, metals, non-metals and their compounds in peat), degree of metamorphism of the fossil coal and so on;

— component composition, procedure of synthesis and method and degree of activation of the raw material;

— particle size characteristics and initial porosity determined by the production process of the adsorbent (pellets, monolith, powder, *etc*).

Quite a few publications[8, 34, 38, 67, 74, 122, 133–141] present data on the dependence of the specific storage capacity of ANG systems on the packing density of porous materials of various classes and the effect of compaction conditions on the adsorbent porous structure.

The packing density of ACs depends on the procedure and degree of physical or chemical activation. As the degree of activation of a carbon adsorbent (U) increases,[142] the porosity develops, the pore size distribution maximum shifts to wider pores and the density decreases, which simultaneously leads to a decrease in the AC adsorption activity and deteriorates the capacity of ANG systems. The variation of packing density of the carbon fibre-based AC *vs*. degree of burn-off of the starting material (U) upon activation has been reported.[27, 38] An example of such dependence is shown in Fig. 21. It can be seen that the dependence is non-linear, and it can be used to identify the processes involved in the activation. According to Dubinin's data,[142] in the U range from 0% to 25%, burn-off of disordered (amorphous) carbon in the intercrystalline space takes place; the proportion of this material in the precursor subjected to activation is relatively low. This gives rise to primary porosity. Then in the 25%–55% range, structured carbon nanocrystallite layers rigidly connected to each other are burned off, giving rise to the basic structure of micropores of up to 3.0–3.2 nm diameters, and the packing density substantially decreases. During further activation in the U = 55%–75% the range, pore width increases and the areas of mesopores with diameters from 3.0–3.2 to 100–200 nm and macropores with diameters of 100–200 nm and more are formed. Thus, to achieve the maximum adsorption, it is necessary to strictly control the porous structure, apart from adjustment of the packing density.

Most of adsorbents are initially powders or pellets, irrespective of the type and origin; therefore, mechanical pressing is the most obvious procedure for increasing their packing density. The initial parameters used for packing density optimization are most often as follows: particle size composition, type of binder and compaction technology (extrusion, cold or hot pressing and so on). A technique for increasing the packing density by adjustment of the particle size composition of the adsorbent was patented.[134] In another patent,[135] it was shown that the highest packing density of a pelletized adsorbent can be attained by using two sizes of particles related as 7 : 1. Other approaches to the preparation of adsorbents with high packing density are also known. In particular, a patent[136] describes a carbonization process for a monolithic precursor based on Saran carbon, which is able to store up to 180 m^3(STP) m^{-3} of a gas. Zhang *et al.*[67] established a nearly linear correlation between V_f of the ANG system and the packing density of AC samples prepared from sorghum grains chemically activated with orthophosphoric acid.

The practically significant range of pressures for the mechanical pressing of ACs based on carbon fibres is depicted in Fig. 22 *a*.[8] It can be seen that the dependence of packing density on the packing pressure is nearly linear; however, after a certain pressure has been reached, the growth of the packing density considerably slows down. It is important that mechanical pressing of adsorbents is

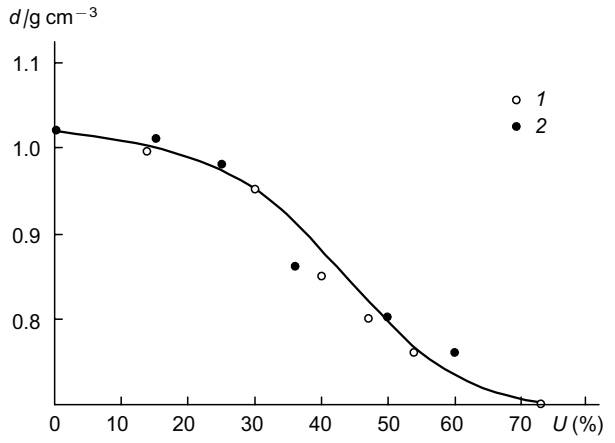


Figure 21. Packing density of AC based on carbon fibres *vs*. degree of activation (burn-off) of the precursor.[38]
(*1*) Carbon dioxide activation; (*2*) steam activation.

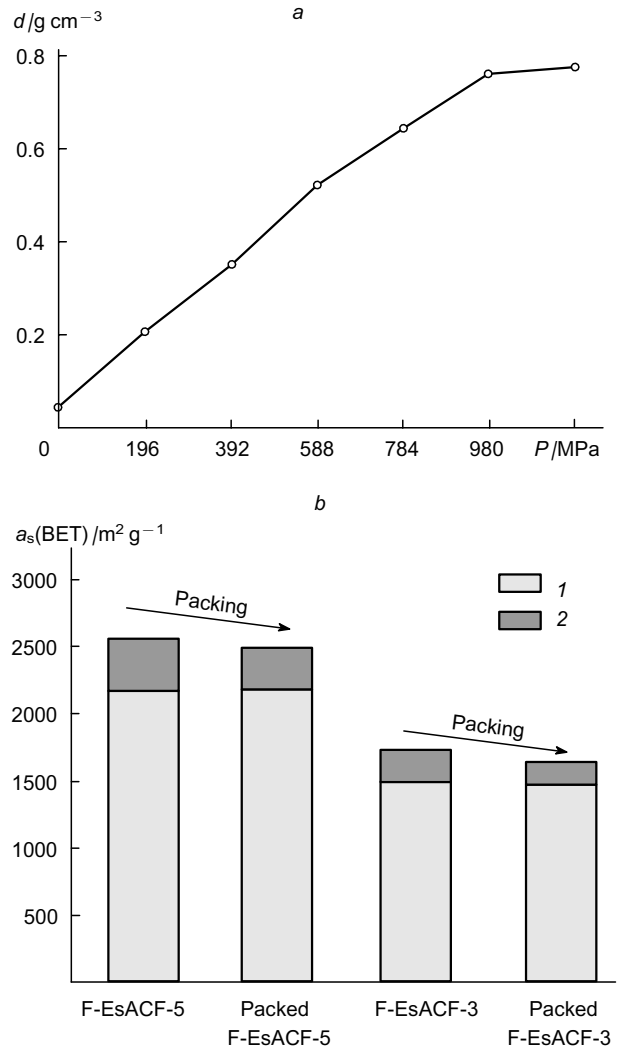


Figure 22. Packing density of AC based on carbon fibres *vs*. packing pressure (*a*) and histograms of packing-induced changes in the specific surface areas of micro- (*1*) and mesopores (*2*) for carbon fibre-based samples F-EsACF-5 and F-EsACF-3 (*b*).[8]

accompanied by partial degradation of their porous structure. The histograms of the specific surface areas of the pores of carbon fibre-based AC are presented in Fig. 22 *b*. It is obvious that pressing induces slight degradation of mesopores, while micropores remain the same and the pore size distribution maximum shifts to narrow pores. Thus, the external mechanical impact not only increases the packing density, but also leads to porosity redistribution. This must be taken into account, especially if the ANG system is to be operated at low pressure.

Let us consider the results of studying unimodal and bimodal AC samples, the latter being prepared by mixing powders of different fractional compositions.[74] The adsorption equilibria of methane were measured by the volumetric method at a pressure of up to 3.5 MPa and a temperature of 293 K. It was shown that pressing of a powdered sample results in a minor degradation of the porous structure manifested as a decrease in the BET surface area and the volume of micropores. In the authors' opinion, due to a greater packing density, the bimodal sample has better characteristics than the unimodal one. The variation of the total specific capacity of the ANG system as a function of packing pressure was elucidated and was found to have a local maximum (Fig. 23). It follows from the obtained results that after a certain packing pressure, the porous structure degradation starts to have a crucial influence on the capacity, since the adsorbent density no longer changes.

Similar results were reported by Kizzie and Dailly,[138] who carried out die pressing of a powdered porous polymer network sample designated as PPN-4. The pressure dependences of the excess and total methane adsorption in PPN-4 at 298 K in the initial and densified states are shown in Fig. 24 *a*. It can be seen that methane adsorption is higher in the initial PPN-4 than in the densified one, which is probably attributable to degradation of the porous structure in a wide pore region. Analysis of the pore size distribution for the adsorbent before and after densification

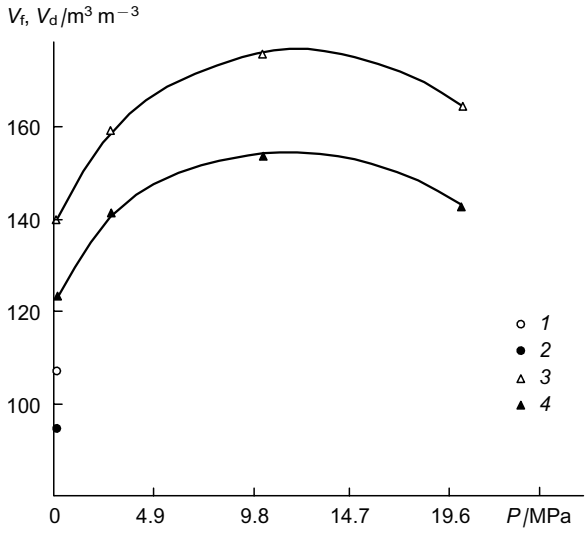


Figure 23. Experimental data (dots) and dependences (continuous lines) of V_f (*1*, *3*) and V_d (*2*, *4*) for an ANG system with anthracite-based AC activated with sodium hydroxide ($r = 3:1$) on the packing pressure of the initial powdered adsorbent at 293 K and 3.5 MPa.[74]
(*1*, *2*) Initial unimodal adsorbent; (*3*, *4*) packed bimodal adsorbent.

(Fig. 24 *b*) showed that pressing resulted in complete redistribution of the porous structure.

Lozano-Castello *et al.*[38] reported a large scale investigation of the methane adsorption in carbon adsorbents prepared from carbon fibres and pitch coal and densified adsorbents based on anthracite. The carbon fibre-based precursors were subjected to physical activation with CO_2 and steam, while anthracite- and pitch coal-based materials were chemically activated with KOH. For production of monolithic samples, the following types of binders were used: poly(vinyl alcohol), sodium salts of humic acids,

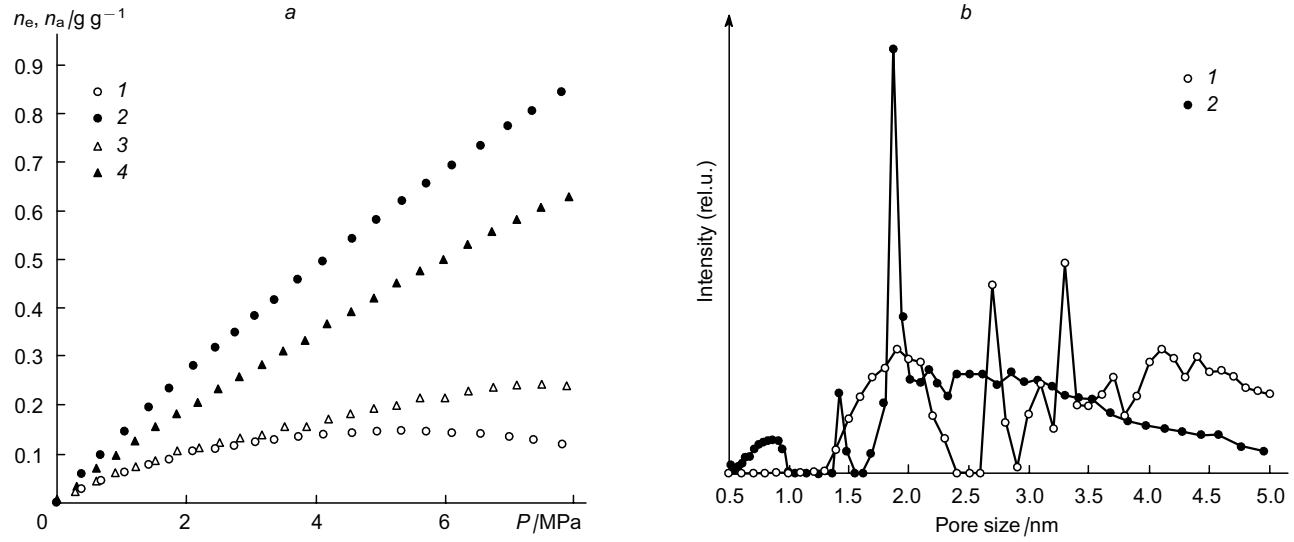


Figure 24. Excess and total methane adsorption *vs.* pressure for a PPN-4 polymer sample at 298 K (*a*) and pore size distribution for this sample in the initial powdered and densified states (*b*).[138]
(*a*) Adsorption: (*1*) excess, powder; (*2*) total, powder; (*3*) excess, densified; (*4*) total, densified; *b*: (*1*) initial powder; (*2*) densified state.

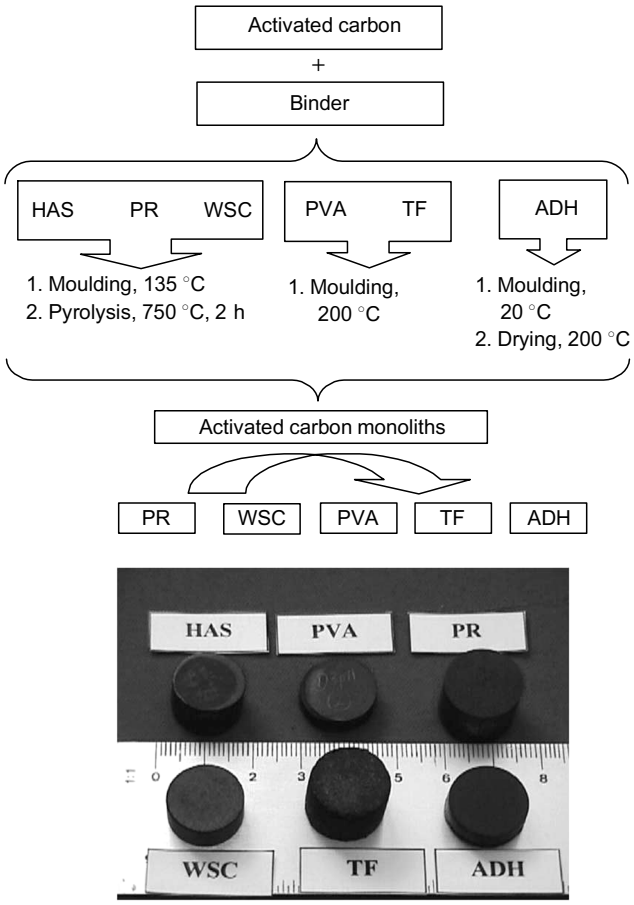


Figure 25. Flow diagram for densification of carbon adsorbents to form monolithic samples with different types of binders: polyvinyl alcohol (PVA), sodium salts of humic acids (HAS), phenolic resin (PR), Teflon (TF), cellulose binder (ADH) and special WSC binder.[38]

phenolic resin, Teflon, a cellulose binder and a special binder of the WSC brand. The flow diagram for the preparation of laboratory samples of monolithic ACs with different binders is depicted in Fig. 25. The binder is significant, because it affects characteristics of the densified material such as strength, dusting and heat conductivity. It is important that the binder present in the adsorption material should not plug the micropores and deteriorate the kinetic characteristics of the adsorbent. The authors noted [38] that the cellulose-based binder is most appropriate. This conclusion was based on experimental data on adsorption, but no detailed explanation for this finding was given.

Porous carbon structures produced as monoliths should be distinguished as a separate class. Examples of such structures are activated carbons based on carbides.[98, 109, 113, 114, 143] These adsorbents have, from the beginning, a high density and a narrow pore size distribution. Good specific adsorption values were obtained for methane storage systems based on this class of adsorbents,[113, 114] which is due, among other factors, to high packing density in the initial state.

The influence of the packing density on the volumetric storage capacity has been considered.[34] The authors analyzed the target requirements to natural gas storage systems and various causes for the loss of adsorption capacity in the case of laboratory samples of powdered and pelletized adsorbents. It is evident that efficient procedures should be developed for adsorbent powder compaction in order to minimize the adsorption loss. The authors concluded that carbon monoliths should be used in methane storage systems, and this will reduce or (in the ideal case) completely eliminate the losses.

The problem of increasing the AC packing density has been considered in relation to carbon pellets.[116] An activated carbon prepared from zeolite raw material with impregnated furfural was studied. The precursor was densified by hot pressing, which increased the packing density from 280 to 980 kg m^{-3}. The authors concluded that hot pressing has a specific effect on the porous structure, namely, mesoporous areas collapse and thus the pore size distribution changes. The densified sample possessed good mechanical strength, which was attributed to the formation of graphite nanocrystallites of approximately the same shape and size during the synthesis.

4.2. Effect of the moisture content of carbon adsorbents on the methane storage efficiency

Water present in natural gas can affect its adsorption. Under certain conditions, water may increase the adsorption capacity of the adsorbent. An approach to increasing the adsorption capacity of ACs for methane by wetting has been considered.[84, 144] It was found that for methane storage in a wet carbon adsorbent, the pore size should correspond to the size of methane hydrates (1.6–2.8 nm). This circumstance was taken into account in the synthesis of AC samples from corn cobs. Carbonization was carried out at 673 K for 30 min in a nitrogen atmosphere and the subsequent potassium hydroxide activation was conducted at 1123 K for 1.5 h. Prior to methane injection, the adsorbent was impregnated with water up to a content of 0.2 to 3.35 g g^{-1}.

The pressure dependences of methane adsorption at 275 K for the AC samples with different water contents are shown in Fig. 26 *a*, and the dependence of methane adsorption on the water content (R_w) of the AC at the same temperature is presented in Fig. 26 *b*. The authors [84] demonstrated that the pore volume and size are the key values that affect the capacity, which was much lower before pore size optimization. By wetting the carbon adsorbent up to a water content of 3.5 g g^{-1}, one can attain the volumetric methane storage capacity of 204 m^3 m^{-3} at 275 K and 9 MPa. According to calculations, pore size optimization under these conditions could result in a unique storage capacity of 290 m^3 m^{-3}; however, this value can hardly be attained in practice.

It should be mentioned that this approach requires additional energy expenditure for maintaining the storage system at a specified temperature. A change of the temperature may induce destruction of gas hydrates in adsorbent micropores, which would violate the operation conditions of the ANG system, cause a considerable decrease in the adsorption capacity for methane and bring about the risk of delivering wet gas to the consumer.

4.3. Thermodynamic conditions of operation of adsorption systems

Casco *et al.*[42] synthesized ACs from plant raw materials and polymers and measured their adsorption characteristics for

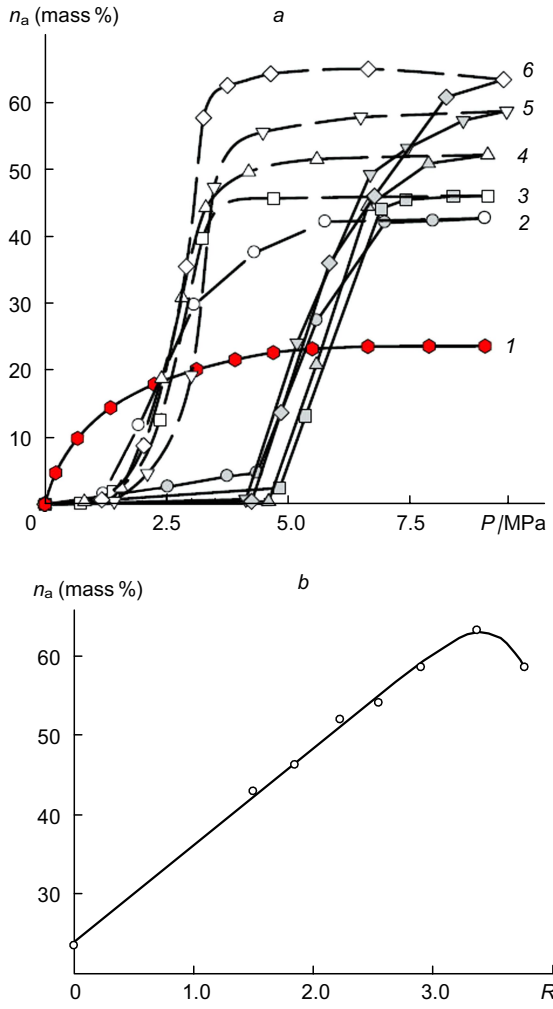


Figure 26. Methane adsorption *vs.* pressure (*a*) and water content (*b*) for corn cob-based carbon adsorbent at 275 K.[84]
(*a*) R_w/g g^{-1}: (*1*) 0; (*2*) 1.5; (*3*) 1.84; (*4*) 2.15; (*5*) 3.75; (*6*) 3.35; continuous lines and dark dots correspond to adsorption; dashed lines and light dots correspond to desorption.

methane. The olive stone raw material (sample LMA405) was first subjected to carbonization at 773 K in an inert atmosphere, then mixed with KOH in 5 : 1 ratio for activation and activated in a horizontal furnace at 1073 K for 2 h.

Two mesophase pitches were used for the thermochemical synthesis of adsorbents, which were labelled as LMA738 and LMA726; the pitches were mixed with KOH in 8 : 1 and 6 : 1 ratios, respectively, and activated at 1073 K for two hours, then washed with 10% HCl and dried at 383 K. The resulting samples had high BET specific surface areas of micropores and micropore volumes determined from the nitrogen adsorption data in terms of the theory of volume filling of micropores.

Sample	LMA405	LMA738	LMA726
a_s(BET) /m^2 g^{-1}	3551	3290	3425
W_0 /cm^3 g^{-1}	1.00	1.10	1.11

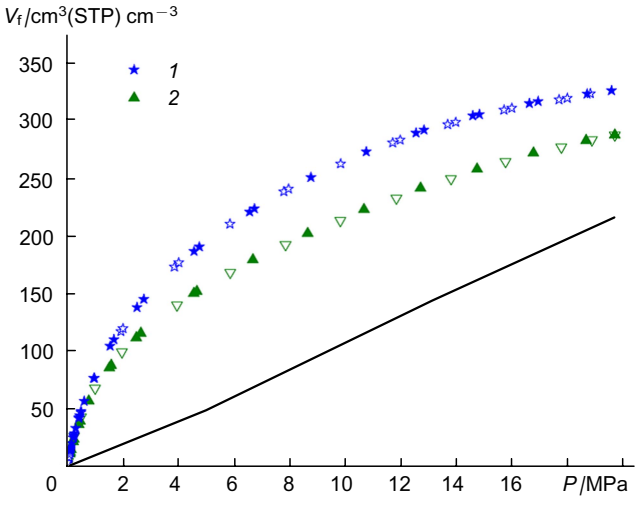


Figure 27. Total specific capacity of the methane storage system based on the adsorbents LMA738 (*1*) and LMA405 (*2*) at a temperature of 298 K and pressures up to 20 MPa (dark dots correspond to adsorption and light dots correspond to desorption) and of the CNG system (continuous line).[42]

The authors[42] noted that, despite the highest specific surface area of the LMA405 sample, the specific capacity of the ANG system with this adsorbent did not exceed 130 m^3 m^{-3} at 3.5 MPa and 298 K, whereas in the case of LMA738 and LMA726, these values were 160 and 150 m^3 m^{-3}, respectively, which attests to the crucial role of the pore size distribution. The authors made an important conclusion that the thermodynamic parameters in the DOE requirements should be revised. Indeed, it follows from Fig. 27 that the maximum performance of ANG systems indicated by the V_f value is attained at >3.5 MPa. For example, the ANG system with the LMA738 adsorbent can efficiently operate at 10 MPa.

Doubts about the adequate choice and targeting towards thermodynamic conditions presented in the DOE requirements were also expressed by other authors.[76, 145]

It was shown[76] that the excess methane adsorption in carbide-based AC samples is maximized at a pressure of about 10 MPa; hence, the maximum efficiency of the adsorption storage also shifts towards higher pressures. The methane adsorption properties of ACs prepared from plant raw materials, peat, furfural, phenol formaldehyde resin and silicon carbide are analyzed in a review.[146] A considerable difference was found between the specific storage capacities of different ACs, and it was shown that every system has its own position of maximum efficiency (Fig. 28). It can be seen that silicon carbide- and peat-based adsorbents have a ΔV_f maximum at 273 K in the pressure range of 3–4 MPa, while in the case of polymer-based adsorbents, the maximum is shifted to 4.5–5.5 MPa. In the authors' opinion, the adsorbent should be chosen considering the thermodynamic conditions of operation of these systems. In view of the intended applications of ANG systems (ranging from on-board systems for motor vehicles to large gas terminals), this concept is quite justified.

Men'shchikov *et al.*[110] addressed the thermodynamic aspects of ANG systems based on carbons prepared from various raw materials including peat, silicon carbide, coco-

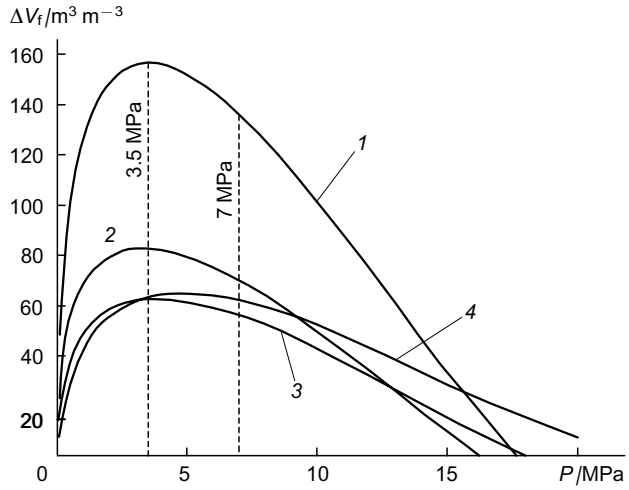


Figure 28. Pressure dependence of the absolute efficiency of a methane adsorption storage system at 273 K for adsorbents based on silicon carbide (*1*), peat (*2*), furfural (*3*) and phenol formaldehyde resin (*4*).[146]

nut shells, polymers and so on. A universal parameter, density of the integral heat of adsorption, was introduced

$$\Omega = \frac{Q}{W_0} \tag{9}$$

where Q is the integral heat of adsorption found for a particular system. Being guided by the Ω value, one can choose the most efficient adsorbents for methane storage systems. The highest integral heats of methane adsorption were found for the AUK (314.75 J cm^{-3}) and PAU-10 activated carbons (312.56 J cm^{-3}) at a pressure of 7 MPa and a temperature of 273 K. Also, a nearly linear relationship was elucidated between Ω and the characteristic

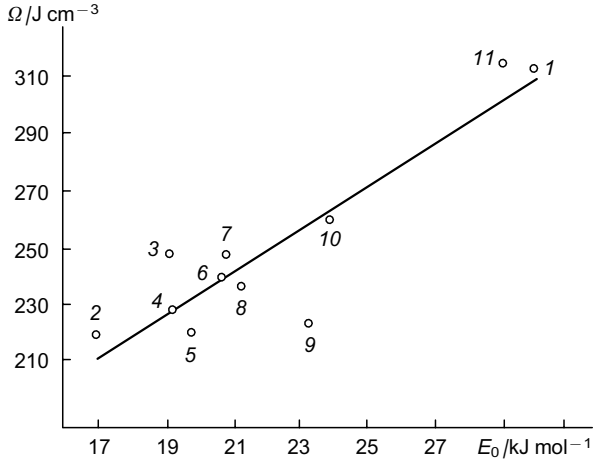


Figure 29. Correlation between the Ω and E_0 values for various adsorbents.[110]
Adsorbents: (*1*) PAU-10; (*2*) AU-3; (*3*) AU-6; (*4*) AU-2; (*5*) AU-1; (*6*) AU-4; (*7*) FEN; (*8*) AU-5; (*9*) FAS-464; (*10*) AU-7; (*11*) AUK. The continuous line is the linear approximation of $\Omega(E_0)$.

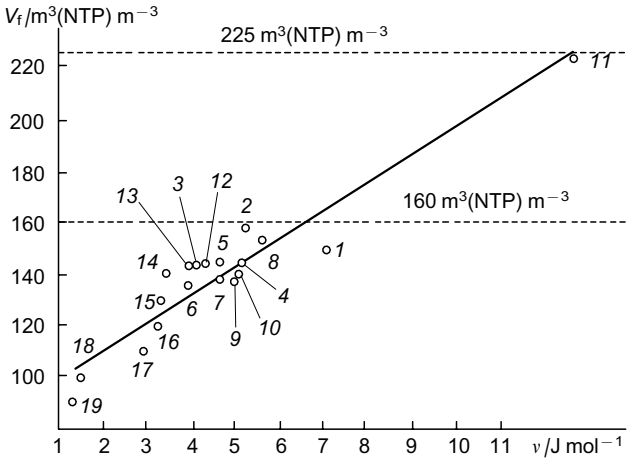


Figure 30. Specific volume of stored methane at 7 MPa as a function of structural and energetic parameter v.[110]
(*1*) PAU-10; (*2*) AU-3; (*3*) AU-6; (*4*) AU-2; (*5*) AU-1; (*6*) AU-4; (*7*) FEN; (*8*) AU-5; (*9*) FAS-464; (*10*) AU-7; (*11*) AUK; (*12*) ART-2; (*13*) AG-OS; (*14*) ART-1; (*15*) AR-B; (*16*) AR-A; (*17*) AR-B; (*18*) AG-PR; (*19*) BAU; the continuous line is the linear approximation of $V_f(v)$.

adsorption energy of the standard benzene vapour (E_0) (Fig. 29).

The density of integral heat of adsorption characterizes a particular microporous adsorbent, but the degree of dispersion and the position within the methane storage system are also important for efficient storage. For describing the storage efficiency, it is reasonable to use the so-called structural and energetic parameter of the adsorbent–adsorbate system

$$v = E_0 W_0 d \tag{10}$$

which takes into account the packing density of the adsorbent (Fig. 30).

The results obtained by Men'shchikov *et al.*[110] can be used to calculate the optimal v values for various ACs with known standard parameters W_0 and E_0 in the supercritical temperature region. This approach seems useful for calculation of the heats of adsorption in the systems of adsorption storage and in heat recovery systems.

5. Theoretical approaches to optimization of the properties of methane–carbon adsorbent adsorption systems

5.1. Numerical modelling

The numerical modelling methods are important for prediction and verification of experimental results. Each method has its own limitations. The achievements in the computer technology substantially enhanced the quality of numerical experiments. However, because of the large number of adsorbate molecules that are simultaneously analyzed in the system and corrected force field parameters, numerical modelling remains more labour-consuming than the analytical methods based on thermodynamic models such as TVFM. Meanwhile, any mathematical model is often based on much more assumptions and approximations than used in a numerical experiment. In any case,

analytical investigations based on mathematical models and numerical experiments often give a key for understanding of physical processes and for the choice of optimal concepts.

Quite a number of studies of this type have appeared in recent years in the field of methane storage. This is determined, first of all, by the necessity to search for new storage materials that would be more efficient regarding both capacity and energy characteristics. In addition, numerical modelling can serve to identify the optimal parameters of the methane adsorption–desorption processes and determine the structure and energy characteristics most appropriate for a particular task.

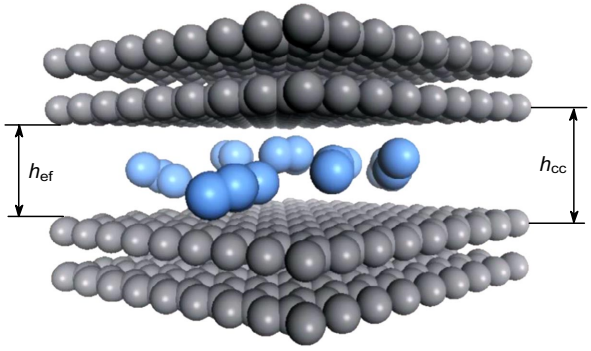


Figure 31. Slit-shaped pore model with walls formed by two carbon layers.[145]
h_{cc} is the pore width, h_{ef} is the effective pore width.

5.1.1. Numerical modelling of methane adsorption in slit-shaped micropores

The slit-shaped pore model for ACs has a physical substantiation considering the pore formation in the adsorbent synthesis. During the activation, successive burn off of carbon layers in carbon nanocrystallites takes place, resulting in pore formation. By varying the methods and conditions of activation, one can generate pores of different width and, hence, adsorbents with different adsorption activity.

The key parameters of a slit-shaped pore are as follows: the width defined as the distance between the centres of carbon atoms located in the planes that form the pore walls (Fig. 31); the number of carbon layers forming the walls; the efficient width, that is, the free distance between the pore walls. The last-mentioned parameter determines the space accessible for sorption of molecules in the pore.

The first studies dealing with methane adsorption in slit-shaped pores formed by planar hexagonal carbon layers were published by Tan and Gubbins[147] and Matranga *et al.*[22] The authors of the former publication[147] used Monte Carlo simulation and non-local density functional theory to demonstrate that for each temperature of methane adsorption, there exists an optimal pore width that ensures the highest excess adsorption. The optimal width for the temperature of ~273 K should fall in the range of 1.22–1.64 nm. Matranga *et al.*[22] employed numerical modelling to determine the theoretical maximum of the capacity that can be attained for carbon adsorbents with slit-shaped pores.[31] For a monolithic porous AC sample, the maximum capacity was found to be ~209 m^3 m^{-3} at a pressure of 3.4 MPa and a temperature of 298 K. According to this publication, the width h_{cc} equal to 1.14 nm (h_{ef} = 0.8 nm) is the optimal if adsorption takes place at 3.5 MPa and 298 K.

The intermolecular Lennard-Jones potential was used to calculate the methane adsorption in model slit-shaped AC pores and in cylindrical zeolite pores.[24] It was concluded that the optimal AC for methane adsorption at 273 K should have ~1.14 nm wide micropores, while the zeolite pore radius should be ~0.57 nm. These values were obtained for the pressure in the storage system of 3.4 MPa and the minimum pressure of gas delivery of 0.1 MPa. It was noted that for pressures < 3.4 MPa, adsorbents with narrower pores should be preferred. The calculations showed that the potential adsorption activity of zeolites is insufficient, due to the relatively low adsorption energy, and that they are poorly suitable for ANG systems.[24]

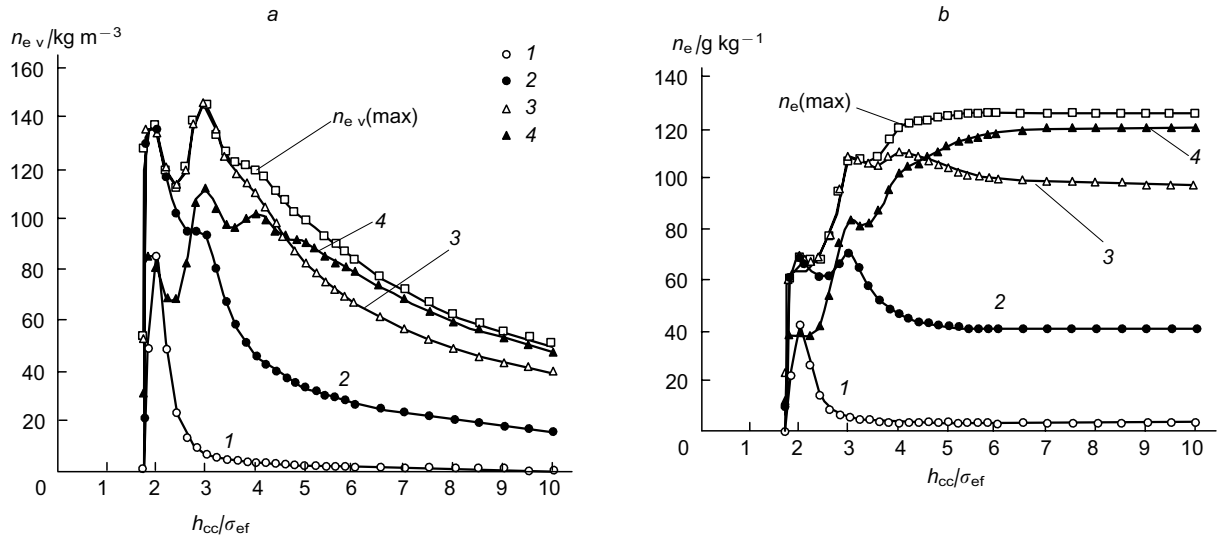


Figure 32. Isobaric dependences of excess methane adsorption in slit-shaped pores of AC *vs.* the parameter h_{cc}/σ_{ef} at 303 K.[31] P/MPa: (*1*) 0.10, (*2*) 1.01, (*3*) 3.55, (*4*) 10.1. $n_{e\,v}$(max), n_e(max) are the maximum possible excess adsorption values measured in grams of adsorbate per unit volume (*a*) and unit mass of (*b*) of the adsorbent, respectively.

Among studies dealing with the search for the optimal slit-shaped pore structure of activated carbons, note the study of Tanaka *et al.*[31] The density functional theory technique was used to calculate excess methane adsorption isotherms for pores of different width (0.381 to 3.81 nm) at different pressures. Using the obtained results, the isobaric adsorption dependences were plotted in the $n_e - h_{cc}/\sigma_{ef}$ coordinates (where $\sigma_{ef} = 0.382$ nm is the diameter of a methane molecule). The results of calculations showed that the highest excess adsorption of methane at 3.55 MPa is attained for the pores with $h_{cc} \approx 1.14$ nm and that the adsorption maximum shifts towards wider pores with increasing pressure. The fluctuations of excess adsorption for h_{cc} values up to 1.5 nm are caused by the fact that the number of layers of methane molecules in a pore is not an integer. Thus for $h_{cc} = 1.14$ nm, the number of layers in a pore reaches two, which provides the maximum excess adsorption. The amount adsorbed in wide slit-shaped pores with $h_{cc} \geqslant 6\,\sigma_{ef}$ is close to that adsorbed on an open surface of graphite. The data on isobaric methane adsorption in model ACs with slit-shaped pores are depicted in Fig. 32. It can be seen that the maximum adsorption shifts to wider pores with increasing pressure in the system.

Kowalczyk *et al.*[148] used the Monte Carlo method to simulate methane adsorption on an open graphite surface and in slit-shaped pores of different width at a temperature of 273 K and a pressure of up to 16 MPa. Local adsorbate density profiles depending on the pore width, which was varied from 0.53 to 9.76 nm, are shown. The surface excess and absolute adsorption isotherms are presented depending on two variables, pressure and effective pore width (Fig. 33). Apart from the adsorption equilibria, the isosteric heats of methane adsorption in various porous carbon structures were calculated (Fig. 34). It was shown that the larger the pore width, the lower the heats of adsorption for low pore fillings; in the case of wide pores, a considerable contribution to the heat of adsorption is made by the formation of associates of adsorbed molecules.

The isosteric heat of methane adsorption (q_{st}) in narrow pores ($h_{ef} = 0.49–0.8$ nm) is nearly constant in the considered pressure range (see Fig. 34). For intermediate pore widths ($h_{ef} = 0.8–1.6$ nm) and medium fillings, the isosteric heat of adsorption increases linearly. This increase is a result of enhancement of adsorbate–adsorbate type interactions. Finally, for the widest pores, the q_{st} value smoothly decreases due to filling of adsorption layers.

An attempt to bring the results of numerical modelling closer to real adsorption systems was made in a study dealing with the variable width of slit-shaped pores of ACs caused by different wall curvature.[149] The variable pore width in the adsorbents may be a consequence of non-uniform activation of the carbon raw materials. The calculations were carried out by the Monte Carlo method for pressures up to 20 MPa. The porous structure was modelled using the atomistic construction of an activated carbon fiber ACF15.

The publication cited above[69] presents the results of integrated analysis of the adsorption characteristics of ACs obtained from coconut shells. The volumetric and numerical methods were used; the adsorbent pores formed by hexagonal graphite layers were assumed to be slit-shaped in the modelling. The authors calculated the adsorbate density in a pore and the absolute and excess adsorption. Pore size distributions were established from the results of numerical

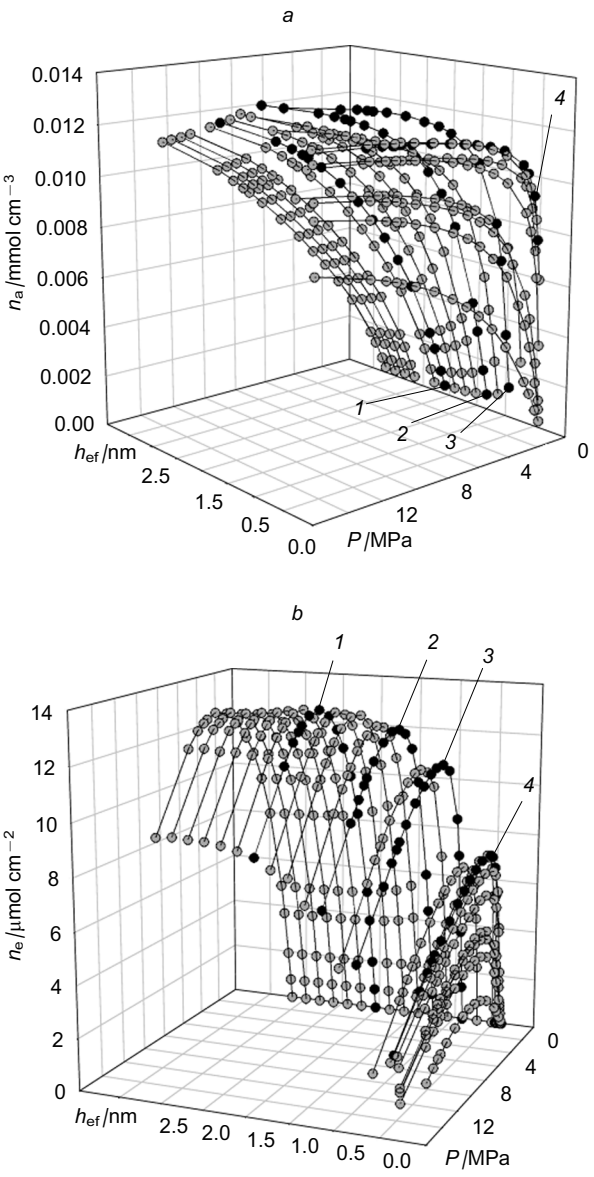


Figure 33. Absolute (*a*) and surface excess (*b*) methane adsorption in the slit-like pores of AC *vs.* pore width and pressure at 273 K. The dark dots designate the isotherms for $h_{ef} = 0.72$ (*1*), 1.14 (*2*), 1.52 (*3*) and 2.2 nm (*4*).[148]

modelling of adsorption of various substances in a model adsorbent. The authors made an ambiguous conclusion that it is impossible to estimate the adsorption activity of an adsorbent towards methane from the adsorbent textural characteristics; it is necessary to take into account also the chemical properties of the surface and other adsorbent characteristics.

The effect of hydrocarbons present in natural gas on the storage behaviour of carbon adsorbents was studied by Lucena *et al.*[145] The Monte Carlo calculations were carried out for a model carbon adsorbent with slit-shaped pores of different width (0.8, 1.85 and 2.79 nm) separated by two graphite layers. The determination of the optimal pore width (1.89 nm) at which the adsorption activity towards methane is not markedly decreased by sorption of other

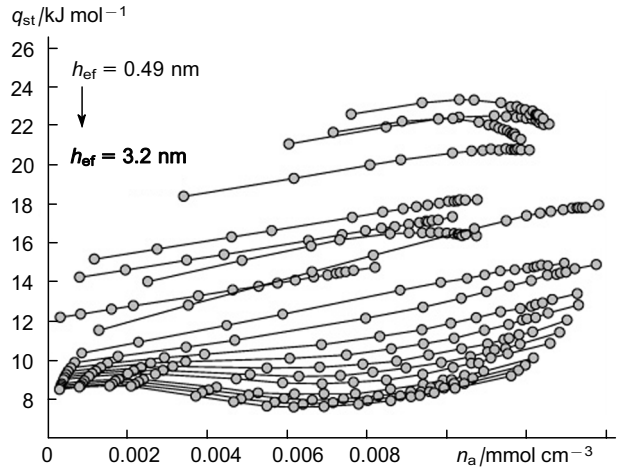


Figure 34. Isosteric heat of methane adsorption in model ACs with pores of different width *vs.* adsorption at 273 K.[148]

hydrocarbons can be regarded as the most significant result of the study of Nguyen *et al.*[149]

According to Kumar *et al.*,[47] the highest methane density is observed at a 0.36 nm distance from the pore wall where the most dense adsorption layer is formed. As molecules move further away from the pore wall, the interaction energy in the adsorbent–adsorbate system sharply decreases and is no longer sufficient to form the second adsorption layer. As a result, the local density of molecules decreases down to a value corresponding to equilibrium pressure in the gas phase. This conclusion was based on the results of calculation of adsorbent–adsorbate interactions in a pore with h_{ef} = 0.86 nm using the Lennard-Jones potential.

The highest density of molecules in the pores is observed when the distance between the pore wall and the molecules corresponds to the minimum of the Lennard-Jones potential for the adsorbent–adsorbate interaction.[3] In this case, the highest adsorption activity would presumably be inherent in the adsorbent with a pore size equal to several diameters of a methane molecule.

Anuchin *et al.*[150] reported the results of the numerical modelling of the methane adsorption in slit-shaped pores of ACs at 273 K and up to 7 MPa pressure; the effective pore width was varied from 0.6 to 1.7 nm and the pore walls were formed by a single layer of carbon atoms. It was found that the highest density of methane is attained in the pores with h_{ef} = 1–1.2 nm.

While considering the methane adsorption in ACs, turn back to the paper of Kumar *et al.*,[47] who determined the theoretical total specific capacity equal to 129 m^3 m^{-3} at 298 K and 3.5 MPa for the pore width corresponding to the maximum methane adsorption according to reported data.[22] As the number of atomic carbon layers forming the pore walls decreases from three to one, the packing density increases to 282 m^3 m^{-3}. It is obvious that this result is impracticable because of the difficulty of synthesis of these adsorbents. It was noted that the highest excess adsorption for this structure is achieved at 6 MPa; therefore, it is more favourable to use ACs at pressures >3.5 MPa.

An important characteristic of slit-shaped pores is the wall thickness. The results of studies of the adsorption of C_1–C_4 alkanes in slit-shaped pores with different wall thickness have been reported.[151] A change in the pore wall thickness was found to have little influence on the adsorption of hydrocarbons heavier than methane and no influence on the adsorption of methane.

Bhatia and Myers[152] showed that the efficiency of methane adsorption storage in AC slit-shaped pores can be evaluated by considering the isosteric heat of adsorption. In the authors' opinion, the optimal q_{st} value is ~16 kJ mol^{-1}; this ensures simultaneously high adsorption and storage properties of the system; the optimal storage temperature is 254 K.

5.1.2. Numerical modelling of methane adsorption in nanotubes

Methane adsorption in carbon nanotubes has been calculated by Monte Carlo methods.[153, 154] The effects of temperature, pressure, nanotube diameter and adsorption energy (with the use of variable parameters of van der Waals interaction) on the methane adsorption in homogeneous open single-walled carbon nanotubes packed in triangular arrays without gaps have been studied.[153] It was found that the use of nanotubes with a diameter of 1.628 nm spaced 1.9 nm apart would provide a volumetric methane storage capacity equal to 96% of the requirements imposed on ANG systems.[30]

A comparison was made of methane adsorption on single-walled boron nitride nanotubes (BNNTs) and carbon nanotubes (CNTs) calculated by density functional theory.[155] Structural optimization for several bonding configurations for a methane molecule approaching the outer surface of BNNT(8,0) or CNT(8,0)‡ demonstrated that the methane molecule is adsorbed predominantly on the CNT surface with a binding energy of 2.84 kcal mol^{-1}. A comparison of nanotubes of different diameters indicated that the ability of methane to be adsorbed on the nanotube outer surface increases with increasing CNT diameter and decreases with increasing BNNT diameter. The introduction of defects into BNNTs markedly enhances the methane adsorption. The possibility for either bilayer or monolayer formation near the nanotube surface was considered. The formation of the second adsorption layer was found to be feasible for CNTs and defective BNNTs. Study of the effect of chemical properties of nanotube surface on methane adsorption provided the conclusion that BNNTs may be unsuitable for natural gas storage.[155]

Numerical methods have been employed to study methane adsorption on three typical carbon nanostructures — graphite, single- and multiwalled carbon nanotubes and nanotube bundles (both within and between the nanotubes).[156] Methane adsorption in other molecular structures, including MOFs, was considered. The following values were estimated: the minimum energies, equilibrium distances, gravimetric and volumetric densities of stored methane, the volume accessible for adsorption, and effects of temperature and pressure on the methane uptake in the analyzed molecular structures.

The same researchers[157] studied packing of methane molecules in single-walled carbon nanotubes and estimated the positions providing the highest packing density. The intermolecular Lennard-Jones potential was used. Zigzag

‡ Hereinafter, the values in parentheses are chiral indices.

and spiral configurations were considered for methane packing into (9,5), (8,8) and (10,10) carbon nanotubes. Analytical expressions for the interaction potential energy were derived for these configurations. In the case of adsorption in (9,5) nanotube with zigzag packing of methane molecules, the potential energy of the system is minimized and the methane molecules form a linear chain along the nanotube axis. In the case of spiral packing, the system potential energy is minimized when the angular spacing is $\sim\pi$ for (9,5) and (8,8) nanotubes and $\pi/2$ for (10,10) nanotubes.

Methane adsorption by nanotube bundles has been considered for triangular arrays of nanotubes with a gap between them.[158–161] The general features of methane adsorption by carbon nanotube arrays have been analyzed.[159] It was shown that monolayer formation in a slit-shaped pore and even on a graphene surface occurs at a lower pressure (and, hence, faster) than that on the nanotube surface. This is due, on the one hand, to the lower adsorbate–adsorbent interaction energy and, on the other hand, to the decrease in this energy caused by the nanotube surface curvature. The highest adsorption energy corresponds to a methane molecule being located inside a small-diameter CNT, which is opened. If the nanotube diameter is relatively large, the adsorption energy is maximized in the gaps between the tubes. It was shown[152] that for adsorption within the nanotubes of various diameters arranged as a bundle without gaps, the requirements to the adsorption methane storage can hardly be met. The authors concluded that a pore space must be generated by positioning nanotubes at particular distances. While considering packing of nanotubes in arrays, the researchers showed that adsorption on the outer surface of CNTs with partly open ends increases more intensively up to a pressure of 4 MPa and then methane molecules are adsorbed on the inner surface of the tubes.[162] It was assumed that open carbon nanotubes positioned at particular distances to form arrays, which additionally increases the porosity, are best suited for methane storage.

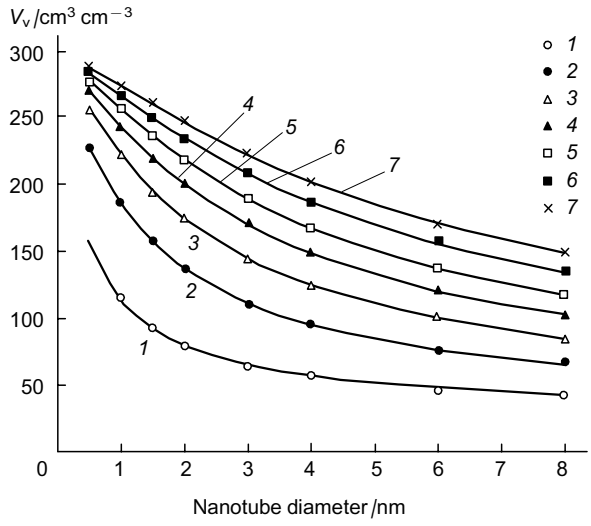


Figure 35. Volumetric methane storage capacity of the modelled supramolecular systems based on open CNTs *vs.* nanotube diameter with distances between the nanotubes of 4 (*1*), 8 (*2*), 12 (*3*), 16 (*4*), 20 (*5*), 25 (*6*), 30 nm (*7*), T = 111.65 K and P = 0.1 MPa.[162]

The prospects of application of carbon nanotube arrays for ANG systems have been discussed[162] (Fig. 35). It can be seen that the amount of methane stored in the intertubular space increases with increasing distance between the tubes, with the tube diameter being invariable, since the volume available for sorption of methane molecules increases. An increase in the nanotube diameter, with the distance between the tubes being invariable, leads to compression of the adsorption space and, consequently, reduces the volumetric capacity for methane. According to calculations, carbon nanotube arrays would be able to meet the DOE requirements in the future.[35]

Interesting results were obtained by combined application of the Monte Carlo simulation and quantum chemical methods to solve the problem of methane storage on CNTs, silicon nanotubes (SiNTs) and silicon carbide nanotubes (SiCNTs) packed into triangular arrays. The methane adsorption was calculated for the temperature range of 273–327 K and pressures up to 9 MPa. The materials were conventionally split into two groups corresponding to small [CNT(11,11), SiNT(7,7), SiCNT(9,9)] and relatively large [CNT(19,19), SiNT(12,12), SiCNT(15,15)] nanotube diameters. The adsorption was studied both inside and outside the nanotubes. The nanotubes were arranged with no additional gaps, being spaced by distances determined by physical interaction between them. For the first group of materials, the methane uptake between the tubes was much more pronounced than that within the tubes below 6 MPa; as the pressure was increased, the uptakes became approximately equal. For the second group of materials, more pronounced differences were observed, particularly, the adsorption between the nanotubes was much higher than within the tubes over the whole range of pressures. For all of the considered systems, the total adsorption under standard conditions was in the range of 160–210 m^3 m^{-3}. The calculations of the volumetric deliverable capacity for methane demonstrated that the material composed of carbon nanotubes with a relatively small diameter, CNT(11,11), meets the requirements to methane storage systems for portable power sources. The volumetric deliverable capacity of this material under standard conditions was 196 m^3 m^{-3} (Fig. 36 *a*) and the heat of methane adsorption was about 16–17 kJ mol^{-1} (Fig. 36 *b*). A decrease in the adsorption temperature by 25 K (down to 273 K) increases the volumetric deliverable capacity of CNT(11,11) to 230 m^3 m^{-3}.

It can be seen from the considered results that carbon nanotubes are most promising for methane storage. The values of volumetric deliverable capacity for methane storage of SiNTs and SiCNTs are substantially inferior to those of CNTs.

Mention should be made of the studies of methane adsorption in other, exotic model microporous carbon materials. For example, methane adsorption has been studied in carbon nanoscrolls and cubic and triangular arrays formed by nanoscrolls.[163] It was shown that at room temperature and 6 MPa pressure, the adsorption can be 13 mmol g^{-1}, which corresponds to the storage level of a high-quality commercial carbon microporous material. The methane storage mechanism by model nanocapsules have been considered.[164, 165] The nanocapsules are opened at elevated temperature. In the authors' opinion, systems of

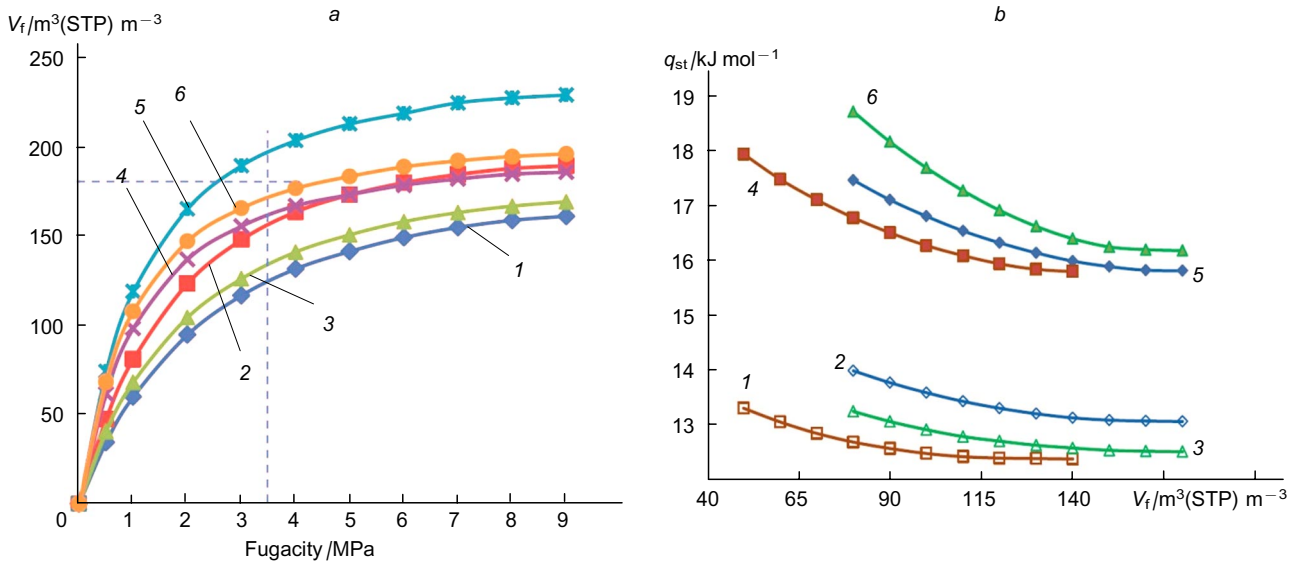


Figure 36. Volumetric capacity of the methane storage system calculated for the excess methane adsorption *vs*. fugacity at 298 K(*a*) and heat of adsorption *vs*. volumetric methane uptake per unit volume of the system (*b*) with adsorbents: (*1*) SiNT(12,12), (*2*) CNT(19,19), (*3*) SiCNT(15,15), (*4*) SiNT(7,7), (*5*) CNT(11,11), (*6*) SiCNT(9,9).[162]

this type will be able to store up to 17.5 mass % methane per capsule at 300 K. Density functional theory was employed to study methane adsorption in aluminium-doped single-walled boron nitride nanotubes (BNNT-Al).[166] The bonding energy between methane molecules and these materials is about 16.53 kJ mol^{-1}. The authors concluded that materials of this type could be applied for methane storage in the future.

Methane storage by silicon nanotube bundles has been studied by numerical methods.[167] Using the Lennard-Jones potential, the interaction energy, molecular forces and the energy of methane molecule capture in a nanotube were determined. The authors deem that silicon nanostructures can be used in methane storage systems at high temperatures, in particular, in the range of 200–400 K.

As materials for methane adsorption, magnesium-impregnated MOF-177 structures packed into fullerenes C_{60} (the full structure designation is Mg–C_{60}@MOF) were used in numerical experiments.[168] The authors claim that such a material will be characterized by a relatively high heat of adsorption and a methane storage capacity of up to 265 m^3 m^{-3} under the conditions defined in the DOE requirements to ANG systems.

The methane storage efficiency was evaluated for porous polymer networks,[169] which represent a class of modern porous materials combining the benefits of cheap stable polymers with the large specific surface area and tunability of the reactivity inherent in metal-organic frameworks. The optimal structure of porous polymer networks for the methane storage was determined by Monte Carlo simulation using a grand canonical ensemble. The best effect was obtained with cooperative methane–methane interactions arising in micropores.

Diamond-like structures are also considered as possible adsorbents for ANG systems.[170] Using density functional theory, methane adsorption and diffusion were calculated for the structures comprising carbon tetrahedra formed according to the diamond pattern and separated by carbon atoms and BN groups and structures in which carbon atoms were partly replaced by silicon and germanium atoms. It was shown that under the DOE conditions, the diamond-like carbon structure shows the maximum volumetric methane storage capacity of 280 m^3 m^{-3}. Unfortunately, the performance of this structure is low due to the slow diffusion of methane. This is why Si- and Ge-containing analogues with better diffusion behaviour were proposed; however, they showed much lower uptake under the same conditions.

Data on methane adsorption by fullerenes and their complexes have been reported.[171–173]. Methane adsorption in fullerene aggregates containing up to six C_{60} molecules was calculated by density functional theory and molecular dynamics methods.[172] It was shown that one aggregate can store up to 58 methane molecules; however, the prospects of these systems for methane storage cannot be evaluated from the presented data. Molecular dynamics simulation of methane adsorption in spherical fullerenes C_{60}, C_{240}, C_{540}, C_{960} and C_{1500} resulted in determination of the optimal radius of a spherical fullerene (0.617 nm) for the insertion of a methane molecule into the fullerene cavity that ensures the lowest potential energy for the interaction between the CH_4 molecule and fullerene surface (0.22 eV).[173] This optimal value for methane encapsulation corresponded to an ideal spherical fullerene larger than C_{60}, but somewhat smaller than C_{240}.

It is noteworthy that the vast majority of numerical experiments simulate carbon microporous materials possessing excellent mechanical (hardness, stability to cyclic loads) and adsorption properties (hydrophobicity, porous structure stability, *etc*.). This refers to potential applicability of these materials in ANG technologies.

5.2. Theoretical methods for studying methane adsorption in carbon adsorbents

The results of theoretical simulation of methane accumulation in model carbon adsorbents (MAC is model active

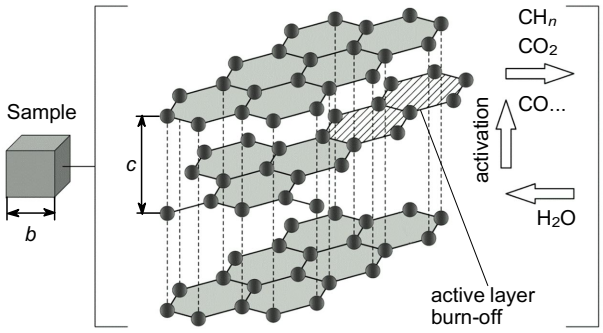


Figure 37. Schematic diagram of steam gas activation of a carbon adsorbent in relation to graphite-like nanocrystallite.[174]
The dark circles designate carbon atoms, c is the distance between hexagonal carbon layers. The carbon atoms are not scaled to size.

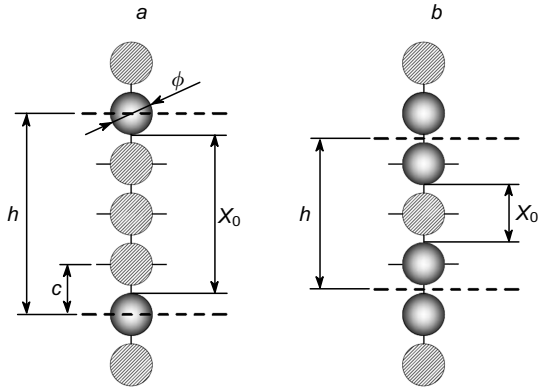


Figure 38. Carbon structure simulation cells (between the dashed lines) with different degrees of activation.[174]
(*a*) Three burnt-off hexagonal carbon layers (hatched circles) out of five layers (MAC3 : 5) and one-layer wall between the pores; (*b*) one burnt-off hexagonal carbon layer (hatched circles) out of five layers (MAC1 : 5) and two-layer wall between the pores; X_0 is the effective micropore width, (*c*) distance between the layers, ϕ is the carbon atom diameter.

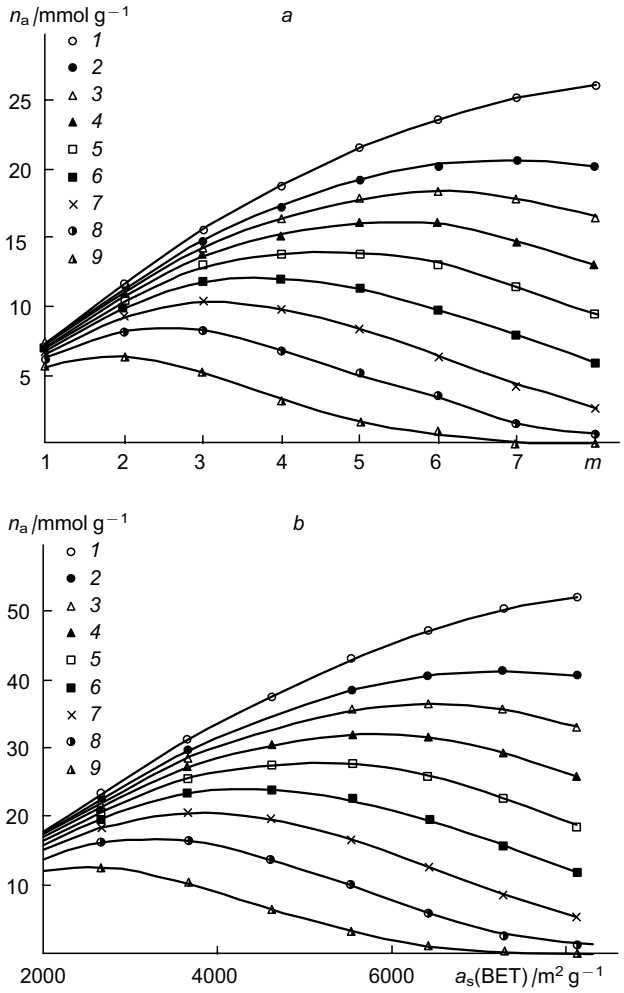


Figure 39. Methane adsorption isobars in the $n_a - m$ coordinates for MAC-2 (*a*) and in the $n_a - a_s$(BET) coordinates for MAC-1 (*b*) at 303 K and pressures of 10 (*1*), 8 (*2*), 7 (*3*), 6 (*4*), 5 (*5*), 4 (*6*), 3 (*7*), 2 (*8*), 1 MPa (*9*).[174]

carbon)) have been reported.[145, 174] The adsorbent was modelled as a graphite cube with porosity arising as a result of successive burn off of carbon layers (Fig. 37).

The structure and energy characteristics were calculated considering a simulation cell representing a nanocrystallite of an activated carbon adsorbent with a specified number of burnt-off layers. The cell simulated a pore between walls formed by one or two layers of carbon atoms packed according to the hexagonal pattern (Fig. 38). Upon variation of the number of burnt-off layers m in the simulation cell with one- (MAC-1) or two-layer (MAC-2) walls, various porous structures of the AC were derived and then the structure and energy characteristics for each system and the theoretical adsorption equilibria were calculated by means of TVFM. Methane adsorption isobars at 303 K plotted *vs.* the number of burnt-off layers for MAC-2 model structures are presented in Fig. 39 *a* and those plotted *vs.* the calculated BET surface area are in Fig. 39 *b*. It can be seen that each isobar has a maximum, which shifts towards more activated structures, that is, structures with higher BET surface area. When an additional parameter (temperature) is introduced, the dependence can be depicted as a surface with an adsorption maximum (Fig. 40).

The key results of the study of Men'shchikov *et al.*[174] are adsorption isobars, which have a maximum, the position of which depends on the specified operating conditions. These dependences are of paramount importance: they demonstrate that to attain the highest adsorption capacity of a methane storage system, the porous structure of the adsorbent must correspond to particular operating conditions of the ANG system defined by thermodynamic parameters (P and T). Thus, the conclusion of some researchers stating that increasing specific surface area and volume of the pores would definitely increase the adsorption at any temperature and pressure is, in general case, erroneous. It is noteworthy that the characteristic energy of adsorption depends not only on the pore shape, but also on the chemical state and deformation of the adsorbent surface. These factors should also be considered when choosing an adsorbent.

This statement corresponds to the conclusion[9] that the BET specific surface area cannot serve as a reliable tool for

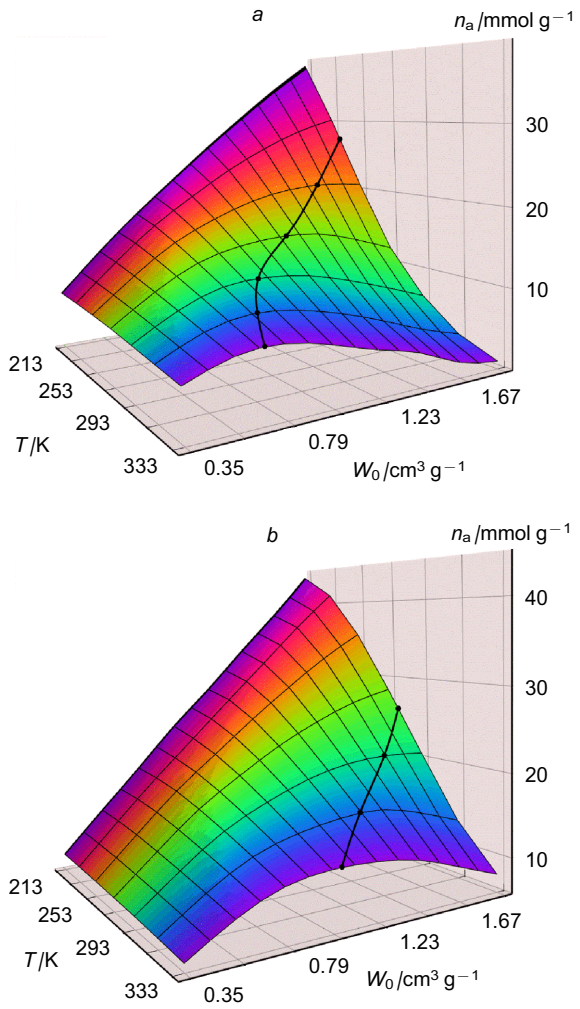


Figure 40. Methane adsorption isobars in the $T-W_0-n_a$ coordinates for MAU-2 type model adsorbents for pressures of 3.5 (*a*) and 7 MPa (*b*).[174]
The points connected by the line on $n_a(W_0, T)_{7MPa}$ and $n_a(W_0, T)_{3.5MPa}$ surfaces correspond to the maximum adsorption values.

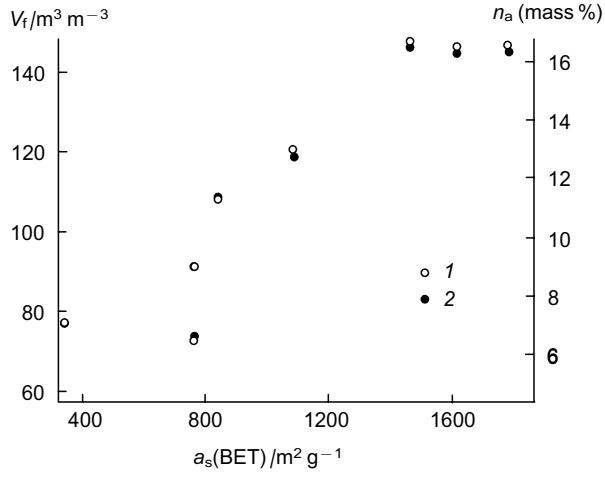


Figure 41. Correlation between the adsorption (*1*), specific methane storage capacity of the system (*2*) and BET specific surface area of activated carbons.[9]

evaluation of the methane uptake of the adsorbent. The correlations of the storage capacity of ANG systems are not linearly increasing (Fig. 41), as stated in many publications. When a_s(BET) > 1500 m^2 g^{-1}, the highest adsorption and specific capacity values for the methane storage system are established.

6. Conclusion

Commercial carbon adsorbents have a number of specific features determined by the surface properties and structure porosity. The carbon surface is electrically neutral, and the adsorption on carbons is mainly determined by dispersion interactions. The porous structure of carbons is characterized by relatively wide pore size distribution. For adsorption of natural gas (methane), micropores, *i.e.*, pores with a size less than 2 nm, have a crucial significance. A distinctive feature of all carbon adsorbents is hydrophobicity. Carbon adsorbents synthesized from polymers, metal and non-metal carbides and nut shells possess high mechanical strength. The textural characteristics of carbon adsorbents do not unambiguously determine the volumetric methane storage capacity. The chemical properties of the micropore surface and the micropore volume affect the energy characteristics and equilibrium values of methane adsorption; therefore, they must be taken into account in the choice of adsorbent for methane storage. During the adsorption, the micropore volume is filled with the adsorbate. In the optimized porous structures, adsorption is enhanced by additional energy resulting from aggregation of adsorbed molecules in micropores. Carbon adsorbents that possess high adsorption energy are most promising for the design of adsorption natural gas (methane) storage systems. There is a broad range of such porous materials classified according to the type of raw material. Apart from the capacity characteristics, choice of the raw material depends on its availability, because large-scale implementation of the technology would require a large amount of the adsorbent. Therefore, fossil coals, especially anthracites, and also peat, wood, wastes of pulp-and-paper and food industries are most promising for the production of adsorbents.

The competing impurities present in natural gas such as heavy hydrocarbons, water, CO_2 and N_2 affect the adsorption of methane, in particular, under cyclic operation, and decrease methane adsorption by 10%–15%. When natural gas contains water, the adsorption capacity of the adsorbent may increase due to the formation of gas hydrates in the pores. The optimal pore size for methane storage in a wet carbon adsorbent should correspond to the dimensions of methane hydrates, that is, should be at least 2.8 nm. From thermodynamic analysis of adsorption processes, it follows that an efficient adsorbent should be chosen considering particular operating conditions defined by pressure and temperature.

The volumetric capacity of activated carbons for methane storage can be improved by increasing the packing density *via* decreasing the space between the pellets in the storage system. However, in this case, too, it is necessary to optimize the packing parameters, including the packing pressure, type of binder, degree of dispersion of the adsorbent, and size and shape of adsorbent particles. It is necessary to control the change in the pore structure upon mechanical pressing. During pressing of carbon adsorbents, slight degradation of mesopores takes place, while the micropores remain unaffected. Thus, the pore size distribution maximum shifts to narrow pores. This conclusion is

important as regards the beneficial effect of the external mechanical impact not only on the bulk density, but also on the formation of porosity, especially if the ANG system is meant for operation at low pressure.

In recent years, modelling of methane adsorption on various porous structures has often been used to develop new efficient (both in the storage capacity and energy characteristics) materials for methane storage. Using numerical modelling, the optimal parameters of methane adsorption and desorption were identified and the structure and energy characteristics most appropriate for this task were determined. According to calculations, the highest excess adsorption of methane at a pressure of 3.55 MPa is attained in ~1.14 nm wide pores; with increasing pressure, the adsorption maximum shifts towards wider pores. The numerical Monte Carlo simulation of methane adsorption in homogeneous open single-walled carbon nanotubes packed in triangular arrays showed that the packing density of materials of this type may correspond to 96% of DOE requirements to adsorption storage systems if the diameter of nanotubes is 1.628 nm and the distance between them is 1.9 nm. The adsorption both inside and outside the nanotubes was investigated. In the case of nanotubes with relatively small diameters, the adsorption between the nanotubes was markedly higher than the adsorption inside the tubes for pressures up to 6 MPa. As pressure was increased, these values became equal. In the case of nanotubes of a larger diameter, the adsorption outside the nanotubes was much higher than inside the tubes over the whole pressure range tested.

Numerical molecular dynamics methods were used to study the methane adsorption on spherical fullerenes C_{60}, C_{240}, C_{540}, C_{960} and C_{1500}. The modelling showed that the optimal minimum energy for methane storage corresponds to a spherical fullerene with a radius of ~0.617 nm, that is, a fullerene with more than 60, but somewhat less than 240 carbon atoms.

Note that the use of numerical methods results, most often, in modelling of new microporous carbon materials. This is caused by their excellent mechanical (hardness, stability to cyclic loads) and adsorption (hydrophobicity, porous structure stability, *etc*.) properties.

The key result of investigation of methane adsorption in model carbon adsorbents with slit-shaped pores using the TVFM is the construction of adsorption isobars that have a maximum depending on the specified thermobaric conditions of system operation. These dependences are fundamental, as they indicate that the maximum adsorption capacity of a natural gas (methane) storage system can be attained if the adsorbent porous structure corresponds to particular operating conditions of the system defined by thermodynamic parameters (P and T). Thus, the traditional point of view that increasing the pore specific surface area and volume would always increase adsorption irrespective of temperature and pressure is, in the general case, erroneous. It is noteworthy that the characteristic energy of adsorption depends not only on the pore structure, but also on the chemical state of the surface and adsorbent deformation. These factors should also be considered for selection of adsorbents.

Figs 5 – 7, 13, 14, 18 – 24, 26, 27, 31 are courtesy of Elsevier; Figs 25, 32 – 34, 36, 41 are courtesy of Springer Nature; and Fig. 16 is courtesy of American Chemical Society.

References

1. C.E.McGlade. *Energy*, **47**, 262 (2012)
2. R.A.Kerr. *Science*, **328**, 1624 (2010)
3. C.Solar, A.G.Blanco, A.Vallone, K.Sapag, in *Natural Gas*. (Ed. P.Potocnik). (InTech, 2010). P. 205
4. Ph.Cleaver, M.Johnson, B.Ho. *J. Hazard. Mater*., **140**, 429 (2007)
5. X.Wang, J.French, S.Kandadai, H.T.J.Chua. *J. Chem. Eng. Data*, **55**, 2700 (2010)
6. L.Wang, H.Gardeler, J.Gmehling. *Sep. Pur. Technol*., **12**, 35 (1997)
7. G.Y.Yevi, R.E.Rogers. *J. Energy Res. Technol*., **118**, 209(1996)
8. J.S.Im, M.J.Jung, Y.-S.Lee. *J. Colloid Interface Sci*., **339**, 31 (2009)
9. A.Policicchio, E.Maccallini, R.G.Agostino, F.Ciuchi, A.Aloise, G.Giordano. *Fuel*, **104**, 813 (2013)
10. C.Guan, L.S.Loo, K.Wang, C.Yang. *Energy Conv. Manag*., **52**, 1258 (2011)
11. A.Sáez, M.Toledo. *Appl. Therm. Eng*., **29**, 2617 (2009)
12. A.Yu.Tsivadze, O.E.Aksyutin, A.G.Ishkov, A.A.Fomkin, I.E.Men'shchikov, A.A.Pribylov, V.I.Isaeva, L.M.Kustov, A.V.Shkolin, E.M.Strizhenov. *Prot. Met. Phys. Chem. Surf*., **52**, 24 (2016)
13. O.E.Aksyutin, A.G.Ishkov, K.V.Romanov, R.V.Teterevlev, A.A.Fomkin, A.V.Shkolin, A.A.Pribylov, I.E.Men'shchikov, U.Muller, L.Arnold, M.Piontek. *Nauka Tekh. Gaz. Prom*., (4) 67 (2016)
14. H.Furukawa, O.M.Yaghi. *J. Am. Chem. Soc*., **131**, 8875 (2009)
15. A.Golovoy, in *SAE Technical Paper Series of the Conference on Compressed Natural Gas as Motor Vehicle Fuel, Pittsburg, PA, 1983*. P. 831070
16. Patent US 4522159 (1985)
17. Patent US 4523548 (1985)
18. E.V.Chkhaidze, A.A.Fomkin, V.V.Serpinskii, G.V.Tsitsishvili. *Bull. Acad. Sci. USSR. Div. Chem. Sci*., **34**, 886 (1985)
19. E.V.Chkhaidze, A.A.Fomkin, V.V.Serpinskii, G.V.Tsitsishvili, M.M.Dubinin. *Bull. Acad. Sci. USSR. Div. Chem. Sci*., **35**, 847(1986)
20. E.V.Chkhaidze, A.A.Fomkin, V.V.Serpinskii, G.V.Tsitsishvili. *Bull. Academ. Sci. USSR. Div. Chem. Sci*., **35**, 252 (1986)
21. L.Mentasty, R.J.Faccio, G.Zgrablich. *Adsorp. Sci. Technol*., **8**, 105 (1991)
22. K.R.Matranga, A.L.Myers, E.D.Glandt. *Chem. Eng. Sci*., **47**, 1569 (1992)
23. M.J.Bojan, R.Slooten, W.Steele. *Sep. Sci. Technol*., **27**, 1873 (1992)
24. R.F.Cracknell, P.Gordon, K.E.Gubbins. *J. Phys. Chem*., **97**, 4 (1993)
25. V.C.Menon, S.Komarneni. *J. Porous Mater*., **5**, 43 (1998)
26. D.F.Quinn, J.A.MacDonald. *Carbon*, **30**, 1097 (1992)
27. J.Alcaniz-Monge, D.Cazorla-Amoros, F.Linares-Solano, A.Oya. *Carbon*, **35**, 291 (1997)
28. K.J.Chang, O.Talu. *Appl. Therm. Eng*., **16**, 359 (1996)
29. A.Grint, S.T.Takagishi. *Adsorbed Natural Gas (ANG) Research Conducted by Atlanta Gas Light Adsorbent Research Group (AGLARG). Final Report*. (1990 – 1993). (Des Planes, IL: Gas Research Institute, End-Use Technology Development Division, 1994)
30. T.Burchell, M.Rogers, in *SAE Technical Paper Series. Goverment Industry Meeting, Washington, DC, 2000*. N 2000-01-2205

31. H.Tanaka, M.El-Merraoui, W.A.Steele, K.Kaneko. *Chem. Phys. Lett.*, **352**, 334 (2002)
32. K.Seki. *Chem. Commun.*, 1496 (2001)
33. S.Noro, S.Kitagawa, M.Kondo, K.Seki. *Angew. Chem., Int. Ed.*, **39**, 2081 (2000)
34. B.P.Prajwal, K.G.Ayappa. *Adsorption*, **20**, 769 (2014)
35. *MOVE Program Overview*. Advanced Research Project Agency, US DOE, 2012; https://arpa-e.energy.gov/sites/default/files/documents/files/MOVE Program Overview.pdf
36. T.L.Cook, C.Komodromos, D.F.Quinn, in *Carbon Materials for Advanced Technology*. (Ed. T.D.Burchell). (Oxford: Elsevier Science, 1999). P. 269
37. T.D.Burchell, in *NATO Science Series E: Design and Control of Structure of Advanced Carbon Materials for Enhanced Performance*. (Eds B.Rand, S.P.Appleyard, M.F.Yardim). (Amsterdam: Springer, 2001). P. 295
38. D.Lozano-Castelló, J.Alcañiz-Monge, M.A.de la Casa-Lillo, D.Cazorla-Amorós, A.Linares-Solano. *Fuel*, **81**, 1777 (2002)
39. Y.Sun, C.Liu, W.Su, Y.Zhou, L.Zhou. *Adsorption*, **15**, 133 (2009)
40. T.A.Makal, J.-R.Li, W.Lu, H.-C.Zhou. *Chem. Soc. Rev.*,**41**, 7761 (2012)
41. F.Chang, J.Zhou, P.Chen, Y.Chen, H.Jia, S.Saad, Y.Gao, X.Cao, T.Zheng. *Asia – Pacific J. Chem. Eng.*, **8**, 618 (2013)
42. M.E.Casco, M.Martínez-Escandell, E.Gadea-Ramos, K.Kaneko, J.Silvestre-Albero, F.Rodríguez-Reinoso. *Chem. Mater.*, **27**, 959 (2015)
43. P.-S.Choi, J.-M.Jeong, Y.-K.Choi, M.-S.Kim, G.-J.Shin, S.-J.Park. *Carbon Lett.*, **17**, 18 (2016)
44. Z.Nie, Y.Lin, X.Jin. *Front. Mech. Eng.*, **11**, 258 (2016)
45. U.D.Hamza, N.S.Nasri, J.Mohammed, Z.Abd.Majid, in *MATEC Web of Conferences. 3rd International Conference on Chemical and Biological Sciences, Amsterdam, 2016*. Vol. 60. P. 04011
46. A.Alonso, J.Moral-Vico, A.A.Markeb, M.Busquets-Fité, D.Komilis, V.Puntes, A.Sánchez, X.Font. *Sci. Total Environ.*, **595**, 51(2017)
47. K.V.Kumar, K.Preuss, M.-M.Titirici, F.Rodríguez-Reinoso. *Chem. Rev.*, **117**, 1796 (2017)
48. M.M.Dubinin, in *Progress in Surface and Membrane Science*. (Ed. D.D.Cadenhead). (London: Academic Press, 1975). P. 1
49. *IUPAC. Compendium of Chemical Terminology*. (2nd Ed.). (Comp by A.D.McNaught, A.Wilkinson). (Oxford: Blackwell Scientific Publications, 1997)
50. GOST 2939-63 Gazy. Usloviya dlya Opredeleniya Ob'ema. (Conditions for Determining the Volume). allgosts.ru/17/060/gost_2939-63
51. J.D.Wright, A.N.Johnson, M.R.Moldover. *J. Res. Natl. Inst. Stand. Technol.*, **108**, 21 (2003)
52. J.Sun, T.A.Brady, M.J.Rood, C.M.Lehmann. *Energy Fuels*, **11**, 316 (1997)
53. E.M.Strizhenov, A.V.Shkolin, A.A.Fomkin, A.A.Pribylov, A.A.Zherdev, I.A.Smirnov. *Prot. Met. Phys. Chem. Surf.*, **49**, 614 (2013)
54. J.Wegrzyn, M.Gurevich. *Appl. Energy*, **55**, 71(1996)
55. V.B.Fenelonov. *Poristyi Uglerod.* (Porous Carbon) (Novosibirsk: Institute of Catalysis, SB RAS, 1995)
56. C.Song, H.Liu, J.Jiao, D.Bai, W.Zhou, T.Yildirim, Y.He. *Dalton Trans.*, **45**, 7559 (2016)
57. D.P.Bezerra, R.S.Oliveira, R.S.Vieira, C.L.Cavalcante Jr., D.C.S.Azevedo. *Adsorption*, **17**, 235 (2011)
58. J.Wegrzyn, H.Wisemann, T.Lee, in *Post-Conference Proceedings for the Annual Automotive Technology Development Contractor's Coordination Meeting, Dearborn, MI, 1992*. P. 1
59. D.F.Quinn, J.A.MacDonald, K.Sosin. *Am. Chem. Soc. Prepr. (Div. Fuel Chem.)*, **39**, 451 (1994)
60. J.Vermesse, D.Vidal, P.Malbrunot. *Langmuir*, **12**, 4190 (1996)
61. *Elaboration and Applications of Metal-Organic Frameworks, (Series on Chemistry, Energy and the Environment. Vol. 2)*. (Eds S.Ma, J.A.Perman). (Singapore: World Scientific Publishing, 2018)
62. D.L.Peterson, F.Helffrich, R.J.Carr. *Am. Inst. Chem. Eng. J.*, **12**, 903 (1966)
63. R.J.Remick, R.H.Elkins, E.H.Camara, T.Bulicz. *Advanced Onboard Storage Concepts for Natural Gas-Fueled Automotive Vehicles. Technical Report of Institute of Gas Technology*. (Chicago, IL: Institute of Gas Technology, Engineering Research Division, 1984)
64. I.Senkovska, S.Kaskel. *Microporous Mesoporous Mater.*, **112**, 108 (2008)
65. V.M.Mukhin, A.V.Tarasov, V.N.Klushin. *Aktivnye Ugli Rossii*. (Active Coals of Russia) (Moscow: Metallurgiya, 2000)
66. M.S.Balathanigaimani, W.-G.Shim, J.-W.Lee, H.Moon. *Microporous Mesoporous Mater.*, **119**, 47 (2009)
67. T.Zhang, W.P.Walawender, L.T.Fan. *Biores. Technol.*, **101**, 1983 (2010)
68. N.Bagheri, J.Abedi. *Chem. Eng. Res. Des.*, **89**, 2038 (2011)
69. A.A.García Blancoa, J.C.Alexandre de Oliveiraa, R.López, J.C.Moreno-Pirajan, L.Giraldo, G.Zgrablich, K.Sapag. *Colloids Surf., A*, **357**, 74 (2010)
70. A.Arami-Niya, W.M.Ashri Wan Daud, F.S.Mjalli, F.Abnisa, M.S.Shafeeyan. *Chem. Eng. Res. Des.*, **90**, 776 (2012)
71. H.Zhang, J.Chen, S.Guo. *Fuel*, **87**, 304 (2008)
72. F.Yan-Yan, Y.Wen, C.Wei. *Chin. Phys. B*, **23**, 108201(2014)
73. D.Lozano-Castelló, D.Cazorla-Amorós, A.Linares-Solano, D.F.Quinn. *Carbon*, **40**, 989 (2002)
74. A.Celzard, A.Albiniak, M.Jasienko-Halat. *Carbon*, **43**, 1990 (2005)
75. A.Perrin, A.Celzard, A.Albiniak. *Microporous Mesoporous Mater.*, **81**, 31 (2005)
76. E.C.Schrage, L.Borchardt. *Carbon*, **48**, 1707 (2010)
77. S.-H.Yeon, S.Osswald, Y.Gogotsi, J.P.Singerb, J.M.Simmons, J.E.Fischer, M.A.Lillo-Ródenas, Á.Linares-Solano. *J. Power Sources*, **191**, 560 (2009)
78. M.S.Balathanigaimani, H.-C.Kang, W.-G.Shim, C.Kim, J.-W.Lee, H.Moon. *Korean J. Chem. Eng.*, **23**, 663 (2006)
79. A.Ganesan, R.Mukherjee, J.Raj, M.M.Shaijumon. *J. Porous Mater.*, **21**, 839 (2014)
80. R.Gottipati, B.Adiraju, S.Mishra. *IACSIT Int. J. Eng. Technol.*, **4**, 468 (2012)
81. K.Munusamy, R.S.Somani, H.C.Bajaj. *BioResources*, **6**, 537 (2011)
82. N.Ferrera-Lorenzo, E.Fuente, I.Suárez-Ruiz, B.Ruiz. *Chem. Eng. J.*, **250**, 128 (2014).
83. K.Inomata, K.Kanazawa, Y.Urabe, H.Hosono, T.Araki. *Carbon*, **40**, 87 (2002)
84. J.Liu, Y.Zhou, Y.Sun, W.Su. *Carbon*, **49**, 3731 (2011)
85. N.V.Kel'tsev. *Osnovy Adsorbtsionnoi Tekhniki*. (Basics of Adsorption Technique) (Moscow: Khimiya, 1976)
86. B.Liu, W.Wang, N.Wang, (Peter) C.T.Au. *J. Energ. Chem.*, **23**, 662 (2014)
87. D.Adinata, W.M.A.Wan Daud, M.Kh.Aroua. *Fuel Proc. Technol.*, **88**, 599 (2007)
88. A.A.-Niya, W.M.A.Wan Daud, F.S.Mjalli. *Chem. Eng. Res. Des.*, **89**, 657 (2011)
89. K.S.Walton, C.L.Cavalcante Jr., M.D.LeVan. *Braz. J. Chem. Eng.*, **23**, 555 (2006)
90. A.Celzard, J.F.Mareche. *Fuel*, **85**, 957 (2006)

91. D.C.S.Azevedo, J.C.S.Araújo, M.Bastos-Neto, A.E.B.Torres, E.F.Jaguaribe, C.L.Cavalcante. *Microporous Mesoporous Mater*., **100**, 361 (2007)
92. M.J.Prauchner, F.Rodriguez-Reinoso. *Microporous Mesoporous Mater*., **109**, 581 (2008)
93. I.E.Men'shchikov, A.A.Fomkin, A.Yu.Tsivadze, A.V.Shkolin, E.M.Strizhenov, A.L.Pulin. *Prot. Met. Phys. Chem. Surf*., **51**, 493 (2015)
94. A.A.Fomkin, A.V.Shkolin, I.E.Men'shchikov, A.L.Pulin, A.A.Pribylov, I.A.Smirnov. *Measur. Techniq*., **58**, 1387 (2016)
95. I.E.Men'shchikov, A.A.Fomkin, A.B.Arabei, A.V.Shkolin, E.M.Strizhenov. *Prot. Met. Phys. Chem. Surf*., **52**, 575 (2016)
96. S.Sahoo, M.Ramgopal. *Sādhanā – Acad. Proc. Eng. Sci*., **41**, 459 (2016)
97. E.M.Strizhenov, A.A.Zherdev, I.A.Smirnov, A.V.Shkolin, A.A.Fomkin, V.A.Sinitsyn, A.L.Pulin. *Prot. Met. Phys. Chem. Surf*., **50**, 15 (2014)
98. A.V.Shkolin, A.A.Fomkin, V.A.Sinitsyn. *Colloid J*., **70**, 796 (2008)
99. E.Alain, B.McEnaney, O.Kozynchenko, V.Strelko, in *Preprints of Paper-American Chemical Society, Division of Fuel Chemistry*. (Washington, D.C.: American Chemical Society. 2001). P. 881
100. A.Celzard, V.Fierro. *Energy Fuels*, **19**, 573 (2005)
101. W.Djeridi, A.Ouederni, A.D.Wiersum, P.L.Llewellyn, L.El Mir. *Mater. Lett*., **99**, 184 (2013)
102. W.Djeridi, A.Ouederni, S.Bourelly, P.L.Llewellyn, L.El Mir, in *Proceedings of Engineering and Technology*. (Monastir, Tunisie: PET, CIER-2014, 2014)
103. M.Molina-Sabio, F.Rodriguez-Reinoso. *Colloids Surf., A*, **241**, 15 (2004)
104. D.F.Quinn, S.Ragan. *Adsorp. Sci. Technol*., **18**, 515 (2000)
105. L.Giraldo, J.C.Moreno-Piraján. *Mater. Sci. Appl*., **2**, 331 (2011)
106. K.C.Kemp, S.B.Baek, W.-G.Lee, M.Meyyappan, K.S.Kim. *Nanotechnology*, **26**, 385602 (2015)
107. I.Prasetyo, Rochmadi, T.Ariyanto, R.Yunanto. *Indian. J. Chem*., **13**, 95 (2013)
108. Y.Li, T.Ben, B.Zhang, Y.Fu, S.Qiu. *Sci. Rep*., **3**, 2420 (2013)
109. C.Vakifahmetoglu, V.Presser, S.-H.Yeon, P.Colombo, Y.Gogotsi. *Microporous Mesoporous Mater*., **144**, 105 (2011)
110. I.E.Men'shchikov, A.A.Fomkin, A.V.Shkolin, E.M.Strizhenov, D.S.Zaitsev, A.V.Tvardovskii. *Prot. Met. Phys. Chem.Surf*., **53**, 780 (2017)
111. *Vremennyi Tekhnicheskii Reglament* 6-16-28-1473-92. *Proizvodstvo Khemosorbenta Uglerodnogo FAS*. (Provisional Technical Regulations 6-16-28-1473-92. Production of Carbon Chemisorbent FAS) (Elektrostal': EKhMZ, 1992). P. 28
112. N.F.Fedorova, G.K.Ivanyuk, D.N.Gavrilov, in *Uglerodnye Adsorbenty i ikh Primenenie v Promyshlennosti*. (Carbon Adsorbents and Their Use in Industry). (Moscow: Nauka, 1983). P. 20
113. F.Li, Q.Qian, S.Zhang, F.Yan, G.Yuan. *J. Nat. Gas Chem*., **16**, 363 (2007)
114. E.Kockrick, C.Schrage, L.Borchardt, N.Klein, M.Rose, I.Senkovska, S.Kaskel. *Carbon*, **48**, 1707 (2010)
115. S.Urbonaite, J.M.Juárez-Galán, J.Leis, F.Rodriguez-Reinoso, G.Svensson. *Microporous Mesoporous Mater*., **113**, 14 (2008)
116. C.Guan, L.S.Loo, K.Wang, C.Yang. *Energy Convers. Manag*., **52**, 1258 (2011)
117. N.P.Stadie, M.Murialdo, C.C.Ahn, B.Fultz. *J. Am. Chem. Soc*., **135**, 990 (2013)
118. M.K.Antoniou, E.K.Diamanti, A.Enotiadis, A.Policicchio, K.Dimos, F.Ciuchi, E.Maccallini, D.Gournis, R.G.Agostino. *Microporous Mesoporous Mater*., **188**, 16 (2014)
119. E.M.Strizhenov. A.V.Shkolin, A.A.Fomkin, A.A.Pribylov, A.A.Zherdev, I.A.Smirnov. *Khim. Technol*., **14**, 729 (2013)
120. V.S.Samofalov. Candidate Thesis in Technical Sciences, IGI (Fossil Fuels Institute), Moscow, 2004
121. J.Luo, Y.Liu, C.Jiang, W.Chu, W.Jie, H.Xie. *J. Chem. Eng. Data*, **56**, 4919 (2011)
122. A.Perrin, A.Celzard, A.Albiniak, J.Kaczmarczyk, J.F.Mareché, G.Furdin. *Carbon*, **42**, 2855 (2004)
123. M.E.Casco, M.Martínez-Escandell, K.Kaneko, J.Silvestre-Albero, F.Rodríguez-Reinoso. *Carbon*, **93**, 11 (2015)
124. A.V.Shkolin, A.A.Fomkin, A.Yu.Tsivadze, K.M.Anuchin, I.E.Men'shchikov, A.L.Pulin. *Prot. Met. Phys. Chem. Surf*., **52**, 955 (2016)
125. A.Yamashita, Y.Mori, T.Oshima, Y.Baba. *Carbon*, **76**, 469 (2014)
126. A.Feaver, G.Cao. *Carbon*, **44**, 590 (2006)
127. M.Namvar-Asl, M.Soltanieh, A.Rashidi. *Energy Convers. Manag*., **49**, 2478 (2008)
128. S.Kayal, A.Chakraborty. *Chem. Eng. J*., **334**, 780 (2018)
129. R.B.Rios, M.Bastos-Neto, M.R.Amora Jr., A.E.B.Torres, D.C.S.Azevedo, C.L.Cavalcante Jr. *Fuel*, **90**, 113 (2011)
130. J.Romanos, T.Rash, S.A.Dargham, M.Prosniewski, F.Barakat, P.Pfeifer. *Energy Fuels*, **31**, 14332 (2017)
131. I.I.El-Sharkawy, M.H.Mansour, M.M.Awad, R.El-Ashry. *J. Chem. Eng. Data*, **60**, 3215 (2015)
132. M.Abdollahi, E.N.Lay, E.Sanjari. *Energy Proc*., **141**, 332 (2017)
133. Patent US 4972658 (1990)
134. Patent US 5094736 (1992)
135. Patent US 5308821 (1994)
136. Patent US 5071820 (1991)
137. J.P.Marco-Lozar, M.Kunowsky, J.D.Carruthers, Á.L.Solano. *Carbon*, **76**, 123 (2014)
138. A.C.Kizzie, A.Dailly, L.Perry, M.A.Lail, W.Lu, T.O.Nelson, M.Cai, H.-C.Zhou. *Mater. Sci. Appl*., **5**, 387 (2014)
139. M.Beckner, A.Dailly, in *Proceeding of the 13th International Conference on Clean Energy (ICCE-2014), Istanbul, 2014*. P. 294
140. M.Molina-Sabio, C.Almansa, F.Rodriguez-Reinoso. *Carbon*, **41**, 2113 (2003)
141. J.P.Marco-Lozar, M.Kunowsky, F.Suárez-García, J.D.Carruthers, A.Linares-Solano. *Energy Environ. Sci*., **5**, 9833 (2012)
142. M.M.Dubinin, in. *Uglerodnye Adsorbenty i ikh Primenenie v Promyshlennosti*. (Carbon Adsorbents and Their Use in Industry). (Moscow: Nauka, 1983). P. 100
143. A.Shahtalebi, A.H.Farmahini, P.Shukla, S.K.Bhatia. *Carbon*, **77**, 560 (2014)
144. M.J.D.Mahboub, A.Ahmadpour, H.Rashidi, N.Jahanshahi. *Energy Sources, Part A*, **38**, 75 (2016)
145. S.M.P.Lucena, V.A.Gomes, D.V.Goncalves, P.G.M.Mileo, P.F.G.Silvino. *Carbon*, **61**, 624 (2013)
146. I.E.Men'shchikov, A.A.Fomkin, A.Y.Tsivadze, A.V.Shkolin, E.M.Strizhenov, E.V.Khozina. *Adsorption*, **23**, 327(2017)
147. Z.Tan, K.E.Gubbins. *J. Phys. Chem*., **94**, 6061 (1990)
148. P.Kowalczyk, H.Tanaka, K.Kaneko, A.P.Terzyk, D.D.Do. *Langmuir*, **21**, 5639 (2005)
149. T.X.Nguyen, N.Cohaut, J.-S.Bae, S.K.Bhatia. *Langmuir*, **24**, 7912 (2008)
150. K.M.Anuchin, A.A.Fomkin, A.P.Korotych, A.M.Tolmachev. *Prot. Met. Phys. Chem. Surf*., **50**, 173 (2014)

151. S.M.P.Lucena, D.V.Gonçalves, P.G.M.Mileo, C.L.Cavalcante Jr. *Adsorption*, **18**, 113 (2012)
152. S.Bhatia, A.Myers. *Langmuir*, **22**, 1688 (2006)
153. Y.Li, P.Wang, L.Ai, X.Sang, J.Bu. *Adv. Mater. Res.*, **291**, 490 (2011)
154. S.J.Mahdizadeh, S.F.Tayyari. *Theor. Chem. Acc.*, **128**, 231 (2011)
155. M.D.Ganji, A.Mirnejad, A.Najafi. *Sci. Technol. Adv. Mater.*, **11**, 045001 (2010)
156. O.O.Adisa, B.J.Cox, J.M.Hill. *Nanoscale*, **4**, 3295 (2012)
157. O.O.Adisa, B.J.Cox, J.M.Hill. *Eur. Phys. J., B*, **79**, 177 (2011)
158. A.G.Albesa, E.A.Fertitta, J.L.Vicente. *Langmuir*, **26**, 786 (2010)
159. S.Vela, F.Huarte-Larranaga. *Carbon*, **49**, 4544 (2011)
160. T.Ohba, K.Kaneko, M.Yudasaka, S.Iijima, A.Takase, H.Kanoh. *J. Phys. Chem. C*, **116**, 21870 (2012)
161. A.V.Shkolin, A.A.Fomkin, E.M.Strizhenov, A.L.Pulin. *Prot. Met. Phys. Chem. Surf.*, **50**, 279 (2014)
162. S.J.Mahdizadeh, E.K.Goharshadi. *J. Nanopart. Res.*, **15**, 1393 (2013)
163. X.Peng, J.Zhou, W.Wang, D.Cao. *Carbon*, **48**, 3760 (2010)
164. M.V.Suyetin, A.V.Vakhrushev. *Micro Nano Lett.*, **4**, 172 (2009)
165. A.V.Vakhrushev, M.V.Suyetin. *Nanotechnology*, **20**, 125602 (2009)
166. K.Azizi, K.Salabat, A.Seif. *Appl. Surf. Sci.*, **309**, 54 (2014)
167. O.O.Adisa, B.J.Cox, J.M.Hill. *Micro Nano Lett.*, **5**, 291 (2010)
168. A.W.Thornton, K.M.Nairn, J.M.Hill, A.J.Hill, M.R.Hill. *J. Am. Chem. Soc.*, **131** 10662 (2009)
169. R.L.Martin, C.M.Simon, B.Smit, M.Haranczyk. *J. Am. Chem. Soc.*, **136**, 5006 (2014)
170. M.Haranczyk, L.-C.Lin, K.Lee, R.L.Martin, J.B.Neaton, B.Smit. *Phys. Chem. Chem. Phys.*, **15**, 20937 (2013)
171. A.Kaiser, S.Zottl, P.Bartl, C.Leidlmair. *Chem. Sus. Chem.*, **6**, 1235 (2014)
172. S.Zöttl, A.Kaiser, P.Bartl, C.Leidlmair, A.Mauracher, M.Probst, S.Denifl, O.Echt, P.Scheier. *J. Phys. Chem. Lett.*, **3**, 2598 (2012)
173. O.O.Adisa, B.J.Cox, J.M.Hill. *J. Nanotechnol. Eng. Med.*, **3**, 041002 (2013)
174. I.E.Men'shchikov, A.A.Fomkin, A.V.Shkolin, V.Yu.Yakovlev, E.V.Khozina. *Izv. AKad. Nauk, Ser. Khim.*, 1814 (2018)